Ecological Indicators 189 (2026) 115099

Contents lists available at ScienceDirect

Ecological Indicators

journal homepage: www.elsevier.com/locate/ecolind

Spatiotemporal heterogeneity and varying associations of environmental pollution and carbon reduction synergy in a typical mountainous megacity: a county-level analysis from Chongqing, China

Xiaoju Li [a,d], Luqman Chuah Abdullah [b,c,*], Lichao Nengzi [a,d], Jinzhao Hu [e], Shafreeza Sobri [b], Mohamad Syazarudin Md Said [b], Siti Aslina Hussain [b], Tan Poh Aun [f]

[a] Xichang University, No. 1 Xuefu Road, Anning Town, Xichang City 615000, Sichuan Province, China
[b] Department of Chemical and Environmental Engineering, Faculty of Engineering, University Putra Malaysia, 43400 UPM, Serdang, Selangor, Malaysia
[c] Institute of Tropical Forestry and Forest Products, Universiti Putra Malaysia, 43400, UPM, Serdang, Selangor, Malaysia
[d] Academy of Environmental and Economics Sciences, Xichang University, Xichang 615013, China
[e] Neijiang Normal University, No. 1 Hongqiao Street, Dongxing District, Neijiang City 641100, Sichuan Province, China
[f] SOx NOx Asia Sdn Bhd, 47620, UEP, Subang Jaya, Selangor Darul Ehsan, Malaysia

ARTICLE INFO

Keywords:
Carbon and pollutant synergistic reduction
Coupling coordination degree model
Geographically and temporally weighted regression
Spatiotemporal heterogeneity
Spatiotemporally varying associations

ABSTRACT

Understanding the spatiotemporal heterogeneity of the environmental pollution reduction and carbon reduction (EPRCR) synergy at the district and county level is essential for targeted urban policy. This study investigates the spatiotemporal evolution and influencing factors of EPRCR at the district and county levels in Chongqing, China, from 2017 to 2022. The analytical framework integrates Centroid-Standard Deviational Ellipse analysis, a coupling coordination degree (CCD) model, kernel density estimation, and a geographically and temporally weighted regression (GTWR) model. The results show that: (1) Major air pollutants ($PM_{2.5}$, PM_{10}, NO_2) declined by about 30% but remained above WHO 2021 Air Quality Guidelines (AQGs). (2) Carbon emissions showed strengthening spatial agglomeration, with the centroid oscillating along a southwest-northeast axis; no significant diffusion of high-carbon industries was detected. (3) The CCD of EPRCR increased overall from 0.54 to 0.61, with cold spots persistently located in the main urban industrial belt while hot spots shifted to lower-density peripheral districts. (4) Per capita GDP and technological innovation showed the strongest positive associations with EPRCR synergy, while industrial energy consumption showed the strongest negative association. These findings reveal spatially uneven EPRCR progress, where industrial zones remain locked in a high-emission paradigm and peripheral districts show positive synergy. Based on these results, this study proposes a zoning, classification, and time-based framework to inform targeted reduction policies for carbon and pollution in Chongqing.[1]

1. Introduction

As global warming intensifies, the emission of carbon dioxide and other greenhouse gases continues to grow. This change has led to more frequent extreme weather events, such as heat waves, droughts, and torrential rains, posing a significant risk to ecosystem balance and socioeconomic systems (Chen et al., 2023c, 2023d; Sun et al., 2025a, 2025b; Xiang et al., 2025). At the same time, rapid industrialization and urbanization have led to the massive emission of various pollutants, further creating complex pollution. This severely impacts both the climate system and natural ecosystems, significantly increases the risk of premature mortality among the population, and has become a major constraint on sustainable development (Fang et al., 2022; Haddad et al., 2023; Roswall et al., 2023; Zaller et al., 2023; Zeng et al., 2022).

* **Corresponding author at:** Department of Chemical and Environmental Engineering, Faculty of Engineering, University Putra Malaysia, 43400 UPM, Serdang, Selangor, Malaysia

E-mail address: chuah@upm.edu.my (L.C. Abdullah).

[1] EPRCR: Environmental pollution reduction and carbon reduction; CCD: Coupling coordination degree; GTWR: Geographically and temporally weighted regression; GWR: Geographical weighted regression; GDP: Gross domestic product; WHO: World Health Organization; AQGs: Air Quality Guidelines; CAQI: Comprehensive Air Quality Index; VIF: Variance inflation factor; OLSR: Ordinary Least Squares Regression.

https://doi.org/10.1016/j.ecolind.2026.115099
Received 12 April 2026; Received in revised form 28 May 2026; Accepted 16 June 2026
Available online 22 June 2026

Currently, China's environmental pollution control has entered a bottleneck period, and the pressure to continuously improve environmental quality is enormous. As the world's largest energy consumer, China's urban energy consumption accounts for as much as 85%, exceeding the world average of 18% (China Media Research Institute, 2024). The energy and industrial structures characterized by high carbon emissions and high pollution are the root causes of China's ecological and environmental problems (Chen et al., 2023a, 2023c, 2023e; He et al., 2025; Zhao et al., 2025). Through the phased implementation of diverse environmental policies, China has achieved significant improvements in environmental pollution and made notable progress in the green transformation of its socio-economic system (Du et al., 2021; Guo et al., 2022; Liu et al., 2022a, 2022b; Xian et al., 2024; Zhang et al., 2024; Zou et al., 2023). However, the status of coal as China's primary energy source is unlikely to change in the short term (Fig. S1).

China's coal-dominated energy structure leads to significant emissions of pollutants and greenhouse gases (Chen et al., 2023b, 2023d, 2023e; Jia et al., 2023a, 2023b; Shi et al., 2023; Zhang et al., 2025a, 2025b). In recent years, with rapid industrialization, China's CO_2 emissions have shown a phased upward trend (Fig. S2). This high-emission trajectory not only further exacerbate the pressure of global warming, but also significantly compress the transition time from peak emissions to carbon neutrality for developing countries compared to developed countries. Furthermore, the key provinces for carbon emissions in China during the 2014 to 2023 exhibited a highly concentrated spatial distribution (Fig. S2). Moreover, these provinces are predominantly located in Northern and Northwestern regions, where the energy system is marked by a strong coal dependency and elevated energy consumption intensity. As a major industrial hub in Southwest China, Chongqing's total emissions remain lower than those of the major energy-producing provinces in the North. However, the city exhibits a unique profile shaped by its specific regional context and distinct development trajectory. Overall, northern provinces face greater pressure to reduce existing carbon emissions, whereas Chongqing is pursuing a pathway that simultaneously accommodates emissions growth from new development and implements low-carbon transition measures.

Carbon emissions have a global impact, while environmental pollutants have a localized effect. However, both are highly related to the same source and process, mainly stemming from the combustion of fossil fuels, and exhibiting multiple synergistic effects (Fig. 1) (Meng et al., 2025; Shi et al., 2026; Shi et al., 2023). China's current environmental policy framework includes two interconnected objectives: reversing ecological degradation, and reducing emissions to meet carbon peak and neutrality targets (Dong and Yang, 2024; Guo et al., 2024; Su et al., 2025). The “dual carbon” target has pointed the way for coordinating environmental pollution prevention and control with greenhouse gas emission reduction, and injected new momentum into the long-term improvement of environmental quality (Chen et al., 2023a, 2023c, 2023d; Xu et al., 2024; Zeng and He, 2023). The coordinated reduction of carbon emissions and environmental pollutants has been identified as a policy priority in China. It serves to effectively mitigate the adverse impacts of global warming and safeguard the lives and property of the people (Jia et al., 2024; Meng et al., 2025; Wang et al., 2022; Xian et al., 2024). However, China is currently facing the combined pressures of EPRCR. Therefore, it is imperative to systematically plan and deploy pathways for EPRCR, and to formulate a top-level design and optimization scheme that aligns with actual conditions.

2. Literature review

Cities face pressure from multiple sources during their development, including addressing climate change, strengthening environmental protection, and promoting economic growth (Huynh et al., 2023; Wang et al., 2024). Therefore, investigating the synergistic effects and potential influencing factors of urban EPRCR can contribute to a better understanding of the interactions among urbanization, the environment, and the economy. In recent years, more and more studies have focused on the spatiotemporal heterogeneity, coupling relationship, synergistic governance effect or trade-off relationship of EPRCR synergistic effects (Chen et al., 2023b, 2023c, 2023d; Huang et al., 2023; Yang et al., 2024; Yang and Ran, 2024).

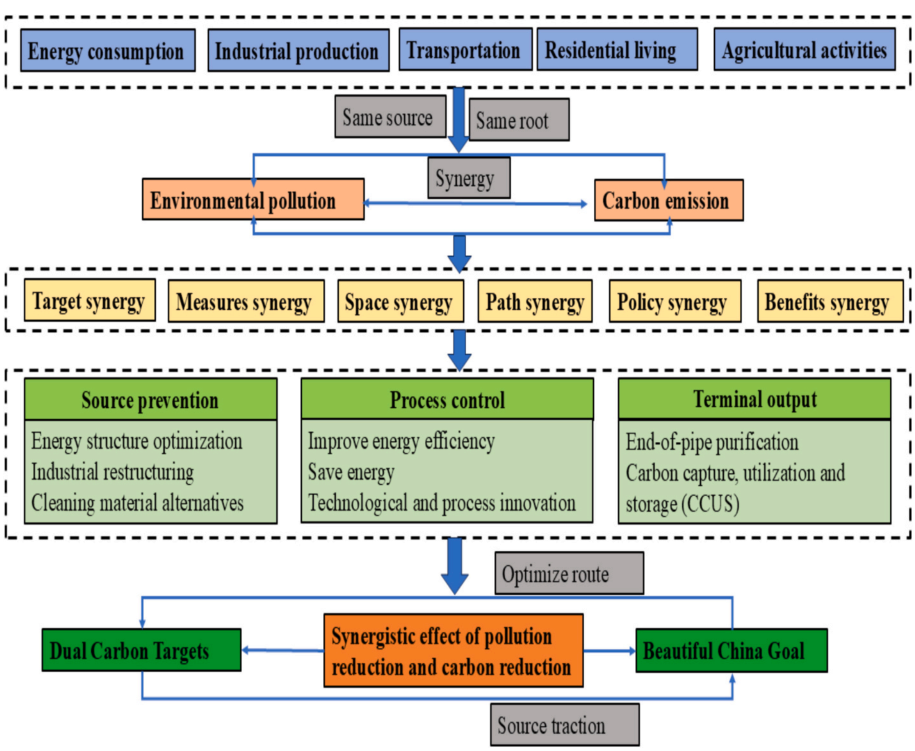

Fig. 1. The theoretical framework for the synergy between EPRCR.

In terms of research scale, the majority of scholars primarily focus on the national (Nie and Lee, 2023; Yi et al., 2023), regional, and industry levels (Chen et al., 2023e, 2023f; Huo et al., 2022; Liu et al., 2024; Ji et al., 2024; Zhang et al., 2025a, 2025b). Regarding methodology, common approaches for investigating the synergy between EPRCR and its spatiotemporal characteristics include GTWR model (Dong et al., 2023), CCD model (Nie and Lee, 2023; Xu et al., 2024; Yang and Ran, 2024), kernel density (Duan et al., 2024; Meng et al., 2025; Ren et al., 2025), spatial autocorrelation (Chen et al., 2023a, 2023b, 2023d; Zhang et al., 2025a, 2025c), the Dagum Gini coefficient, Markov chain and complex system coordination degree model (Meng et al., 2025; Sun et al., 2025a, 2025b; Xie et al., 2024; Yi et al., 2023). For instance, Cao and Yuan (2019) employed a combination of the logarithmic mean Divisia index (LMDI) and geospatial analysis to investigate the drivers of land-use-related CO_2 emissions at the county and district level in Chongqing from 1997 to 2015. Their findings indicated that total energy consumption exerted the most significant influence (Cao and Yuan, 2019). Duan et al. (2024) found that environmental governance investment and government intervention are key drivers of EPRCR by integrating multiple methods such as marginal cost-benefit analysis, spatial kernel density estimation, and geographic detectors (Duan et al., 2024). Liu et al. (2024) used the improved Tapio decoupling principle and the Probit model to assess the synergistic effect of EPRCR across 295 cities in China, pointing out that environmental regulation is the most critical factor in fostering these synergistic effects (Liu et al., 2024).

Furthermore, current research on the influencing factors of synergistic carbon and environmental pollution reduction is mainly divided into comprehensive perspectives and single perspectives. The comprehensive perspective primarily employs econometric models to investigate the potential influencing factors through which economic and social indicators influence the synergistic effects of EPRCR (Chen et al., 2025; Gao et al., 2022; Su et al., 2025; Zou et al., 2023). For example, Zou et al. (2023) used the triple difference method to explore the influencing factors of carbon pollution synergistic emission reduction benefits in various provinces and industries in China, and found that environmental regulations, energy substitution and technological innovation are the main factors (Zou et al., 2023). Through GTWR model analysis, Qin et al. (2023) found that energy consumption structure and industrial structure are the main influencing factors associated with coordinated reduction of $PM_{2.5}$ and CO_2 emissions in Chinese provinces (Qin et al., 2023). On the other hand, a single perspective focuses on the role of specific factors such as low-carbon city projects, carbon trading, and environmental regulations in the synergistic effect of EPRCR (Cui et al., 2020; Gao et al., 2022; Qian et al., 2021). For example, the findings of Dong et al. (2022) and Xian et al. (2024) both indicate that carbon trading policies have a positive synergistic effect on carbon emission reduction and air pollution control. Besides, Chen et al. (2022) confirmed that China's carbon emissions trading system has reduced total carbon emissions and reduced air pollution. Shao et al. (2023) also pointed out that low-carbon policies promote industrial structure upgrading and energy structure optimization, thereby improving the atmospheric environment. In addition, other major related studies on the synergistic reduction of carbon and environmental pollution are detailed in Table S1.

Existing literature has studied EPRCR from different perspectives. These research results have verified that the coordinated governance of carbon and environmental pollution is the most effective and economical means to address the dual pressures of environmental pollution and greenhouse gas emission reduction (Han et al., 2023; Xiang et al., 2025; Yang et al., 2025). Given the significant differences in resource conditions and economic development levels across different regions of China, it is necessary to abandon the “one-size-fits-all” approach and instead adopt more targeted and differentiated measures based on the specific characteristics of each city. Despite the abundance of existing research, the following shortcomings still exist:(1) From a research perspective, most current studies focus on the national, provincial, municipal, and urban cluster levels. Existing research has yet to conduct an in-depth exploration of districts and counties, thereby constraining the level of refinement and precision in policy implementation. (2) In terms of research content, current research on Chongqing focuses more on EPRCR, and there is insufficient discussion on the synergistic effect of EPRCR at the district and county scales. (3) From the perspective of research methods, existing analyses of the influencing factors of EPRCR are mostly based on global regression, which makes it difficult to capture the spatiotemporal nonstationarity of these factors and their local and dynamic changes.

Only by conducting an in-depth analysis of the development of coordinated EPRCR promotion across various districts and counties can we find the right direction to achieve the city's overall goal of green and low-carbon transformation. To circumvent these limitations, this study selected 38 districts and counties in Chongqing as research subjects, and the main research contents included: (1) Using ArcGIS and the centroid-standard deviation ellipse to reveal the spatiotemporal evolution pattern of carbon emissions and air pollutants from 2017 to 2022; (2) The CCD model was used to measure the CCD between EPRCR, and its spatiotemporal correlation characteristics were explored through kernel density analysis and spatial autocorrelation model; (3) Useing the GTWR model to explore the key influencing factors of the synergy between EPRCR. The innovation of this study lies first in its research perspective, which analyzes the spatial effects of EPRCR in typical mountainous megacities from a more detailed district and county perspective, and proposes more precise and targeted recommendations and measures. Secondly, in terms of research methods, multiple models are coupled to form a comprehensive analytical framework of “pattern-process-spatiotemporally varying associations”, which overcomes the limitation of traditional methods that ignore spatiotemporal nonstationarity. This study develops a zoning, classification, and time-based framework to inform carbon and pollution reduction policies for Chongqing. It also provides empirical findings that may be transferable to other mountainous cities in the Yangtze River Economic Belt, pending validation of similar conditions.

3. Methodology

3.1. Study area

Chongqing is located in the eastern part of the Sichuan Basin in southwestern China. With a landscape composed largely of mountains and hills, it is famously referred to as the “Mountain City” (Lu et al., 2022; Tan et al., 2023). The unique topography and climate conditions of low wind speed and high frequency of calm winds result in poor conditions for the dispersion of air pollutants, making it easy for local pollution to accumulate (Feng et al., 2023; Long et al., 2022; Xiang et al., 2025). As an ecological barrier for China's Yangtze River Economic Belt, Chongqing has constructed a “one district and two clusters” urban development pattern. It includes the metropolitan area, the northeastern Chongqing urban cluster, and the southeastern Chongqing urban cluster. This spatial configuration exhibits a notable characteristic—the coexistence of “large cities, large rural areas, large mountainous areas, and large reservoir areas” (Feng et al., 2023; Tan et al., 2023; Xiang et al., 2025).

Furthermore, as one of China's old industrial bases, Chongqing has developed pillar industries such as automobile and electronics manufacturing, and its energy consumption structure is dominated by coal and oil (Harper et al., 2021; Long et al., 2022; Zhang et al., 2025b, 2025c). This results in a dense concentration of carbon emissions and air pollutant emission sources, with complex emission characteristics. Moreover, the districts and counties of Chongqing differ significantly in terms of economic development stage, resource endowment, and functional positioning. The main urban areas have a high concentration of industry and population, while the northeastern and southeastern regions of Chongqing bear the function of ecological protection and conservation (Long et al., 2022; Xiang et al., 2025; Zhang et al., 2025a, 2025c). This heterogeneity provides a natural research sample for revealing the spatial nonstationarity of the spatiotemporal evolution and spatiotemporally varying associations of carbon emissions. In addition, given Chongqing's economic and industrial weight within the Chengdu-Chongqing Economic Circle, the findings of this study may inform understanding of the region's environmental trajectory.

3.2. Methods

To systematically elucidate the spatiotemporal heterogeneity and varying associations of the synergistic effects between EPRCR in Chongqing, this study designed an analytical framework comprising "synergy measurement—spatiotemporal pattern analysis—spatiotempo rally varying associations exploration." First, the spatial characteristics of carbon emissions are analyzed using the centroid standard ellipse method; subsequently, the degree of synergy between EPRCR is measured by integrating the entropy weight method and a CCD model, thereby providing the foundational dependent variable for subsequent spatiotemporal analysis. Secondly, to systematically characterize the spatiotemporal differentiation patterns of synergistic effects, kernel density estimation and spatial autocorrelation analysis were employed to reveal the spatiotemporal evolutionary characteristics of the degree of synergy. Finally, the GTWR model was employed to investigate the associations of various potential influencing factors with the degree of synergy, thereby identifying the primary associated factors.

3.2.1. Entropy weight method

This study selects the entropy weight method to assign weights to various indicators of EPRCR, aiming to minimize and avoid the interference of subjectivity on the evaluation results. In entropy weighting, the weight of each indicator is derived from its information entropy, which quantifies the degree of data dispersion across evaluation unit (Chen et al., 2023b, 2023c, 2023f; Zhang et al., 2025b, 2025c). The specific steps of this method are as follows:

Step 1: Use the range method to standardize the original data to eliminate the influence of different indicator units (Cui et al., 2022a, 2022b; Zhang et al., 2025a, 2025c):

$$\text{Positive indicators}: Y_{ij} = \frac{X_{ij} - \min(X_{ij})}{\max(X_{ij}) - \min(X_{ij})} \tag{1}$$

$$\text{Negative indicators}: Y_{ij} = \frac{\min(X_{ij}) - X_{ij}}{\max(X_{ij}) - \min(X_{ij})} \tag{2}$$

where X_{ij}represents the original value of the i^{th} evaluation object on the j^{th} indicator. $Y_{ij}$is the standardized value. For the case where the standardized value is 0, it is approximated as 0.0001.

Step 2: Calculate the weight of each of the j evaluation indicators in the i^{th} city (Cui et al., 2022a, 2022b; Zhang et al., 2025a, 2025c):

$$P_{ij} = \frac{Y_{ij}}{\sum_{i=1}^{n} Y_{ij}} \tag{3}$$

Step 3: Calculate the information entropy of the j^{th} indicator to reflect the degree of data dispersion (Xu et al., 2024; Zhang et al., 2025b):

$$e_j = -\left(\frac{1}{\ln n}\right)\sum_{i=1}^{n} p_{ij}\ln\left(p_{ij}\right) \tag{4}$$

Step 4: Determine the weight of each indicator based on its entropy value (Xu et al., 2024):

$$w_j = \frac{1 - e_j}{\sum_{j=1}^{n}(1 - e_j)} \tag{5}$$

Step 5: Calculate the carbon reduction or pollution control level (U) for each city (Xu et al., 2024; Zhang et al., 2025a, 2025b):

$$U = \sum_{j=1}^{n} wjY_{ij} \tag{6}$$

3.2.2. Coupling coordination degree model

To quantify the degree of synergy between EPRCR systems, this study introduces a CCD model to calculate the synergy scores for each district and county. The CCD model can simultaneously reflect the collaborative development trend of different subsystems and the overall effect between systems (Chen et al., 2024; Yang and Ran, 2024). First, construct the EPRCR coupling model as shown in Eq. (7) (He et al., 2025; Sun et al., 2025a; Yang and Ran, 2024):

$$C = \sqrt{\left[1 - \sqrt{(U_2 - U_1)^2}\right] \times \frac{U_1}{U_2}} = \sqrt{[1 - (U_2 - U_1)] \times \frac{U_1}{U_2}} \tag{7}$$

where, $U_1$and U_2 represent the standardized values of the two subsystems of PR and CR, respectively. C represents the coupling degree between carbon emissions and pollutant emissions. The value of C is between 0 and 1, and the larger the value, the stronger the interaction between the subsystems. However, even if both subsystems perform poorly, a high degree of coupling may still occur (Wang et al., 2024; Zhang et al., 2025b, 2025c). Therefore, coordination degree must be introduced to assess the overall level of coordination. The CCD model is constructed as shown in Eq. (8) and (9) (He et al., 2025; Lei et al., 2024):

$$T = \alpha U_1 + \beta U_2 \tag{8}$$

$$D = \sqrt{C^* T} \tag{9}$$

T and D represent the degree of coordinated development and the degree of coupling coordination in EPRCR, respectively. The value of D ranges from 0 to 1, with higher values indicating stronger coupling coordination. In addition, α and β represent parameters to be determined. Following the principle of policy parity in China's synergistic pollution-carbon reduction framework – where neither pollution reduction nor carbon reduction is prioritized over the other - the two subsystems are assigned equal weights. Thus, the undetermined parameters are set as $\alpha = \beta = 0.5$, consistent with existing literature (Nie and Lee, 2023; He et al., 2025; Xiang et al., 2025). The specific categories and classification criteria for the CCD are presented in Table 1 (Meng et al., 2025; Xiang et al., 2025; Zhang et al., 2025a, 2025b).

3.2.3. Kernel density estimation

To reveal the evolutionary characteristics of the overall spatial distribution patterns of synergy across the entire region, this study employs the kernel density estimation method to characterize changes in the position, kurtosis, and tailing of the distribution curves. Kernel density estimation is a method that uses continuous density curves to characterize the distribution of random variables and belongs to nonparametric estimation techniques (Meng et al., 2025; Ren et al., 2025; Sun et al., 2025a). Compared with other estimation methods, kernel density estimation has the characteristics of strong robustness and weak

Table 1
Coupling coordination degree classification criteria.

Phase	Model	Couple coordination D
1	Extremely non-coordination	[0,0.1]
2	Severe non-coordination	[0.1,0.2]
3	Moderate non-coordination	[0.2,0.3]
4	Mild non-coordination	[0.3,0.4]
5	Near non-coordination	[0.4,0.5]
6	Near coordination	[0.5,0.6]
7	Primary coordination	[0.6,0.7]
8	Intermediate coordination	[0.7,0.8]
9	Good coordination	[0.8,0.9]
10	Excellent coordination	[0.9,1.0]

model dependence (Ren et al., 2025; Sun et al., 2025a, 2025b). By estimating the probability density of a random variable, the position and shape of the kernel density curve can be used to reveal the dynamic characteristics of the random variable. The density function of the random variable x is expressed as in Eq. (10) (Ren et al., 2025; Sun et al., 2025b):

$$f(x) = \frac{1}{nh}\sum_{i=1}^{n} k\left(\frac{x_i - \overline{x}}{h}\right) \tag{10}$$

In the formula, $x_i$represents the sample data, $\overline{x}$represents the sample mean, n represents the number of sample data, h represents the bandwidth, and K(.) represents the kernel function. The larger the bandwidth, the more sample information is lost; the smaller the bandwidth, the worse the smoothness of the fitted curve (Meng et al., 2025; Ren et al., 2025). The window width determined in this study is based on Silverman's optimal window width method (Sun et al., 2025a, 2025b; Yu and Li, 2025).

The distribution dynamics are estimated using the commonly used Gaussian kernel function, as shown in Eq. (11) (Meng et al., 2025; Yu and Li, 2025):

$$k(x) = \frac{1}{\sqrt{2\pi}}\exp\left(-\frac{x^2}{2}\right) \tag{11}$$

3.2.4. Centroid -standard deviational ellipse

To identify the center, dominant direction, and trends of aggregation or dispersion in carbon emission distribution, this study employs the standard deviation ellipse method to analyze changes in the ellipse's coverage area and the orientation of its major axis. The centroid-standard deviation ellipse method generates ellipses centered on the centroid and with the standard deviation as the axis of distance, to quantitatively reveal the location of geographic element clusters, diffusion range, extension direction and spatial configuration (Deng et al., 2022; Xu et al., 2022). The center of gravity is calculated as shown in Eq. (12) (Xiang et al., 2026; Zhang et al., 2025b, 2025c):

$$\left(\bar{X}_w, \bar{Y}_w\right) = \left(\frac{\sum_{i=1}^{n} w_i x_i}{\sum_{i=1}^{n} w_i}, \frac{\sum_{i=1}^{n} w_i y_i}{\sum_{i=1}^{n} w_i}\right) \tag{12}$$

(x_i, y_i) represents the spatial coordinates of the element, and $w_i$represents the spatial weight，n is the total number of elements.

The distance of center of gravity migration is measured as shown in Eq. (12) (Chen et al., 2023; Xiang et al., 2026):

$$D = H \times \sqrt{(X_m - X_n)^2 - (Y_m - Y_n)^2} \tag{13}$$

In the formula, D is the distance the center of gravity of the research object moves between different years, km; H is a constant, which is a coefficient for converting geographic coordinate units to planar distance, usually take as 111.111; (X_m, Y_m) and (X_n, Y_n) are the geographic coordinates of the center of gravity of the research object in year m and year n, respectively (Chen et al., 2023b; Xiang et al., 2026).

The azimuth measures the angle from true north to the major axis of an ellipse, thereby revealing the dominant directional trend in the spatial arrangement of geographic elements (Eq. 14) (Xiang et al., 2026; Zhang et al., 2025b, 2025c):

$$\tan\theta = \frac{\left(\sum_{i=1}^{n} w_i^2 \widetilde{x}_i^2 - \sum_{i=1}^{n} w_i^2 \widetilde{y}_i^2\right) + \sqrt{\left(\sum_{i=1}^{n} w_i^2 \widetilde{x}_i^2 - \sum_{i=1}^{n} w_i^2 \widetilde{y}_i^2\right) + 4\sum_{i=1}^{n} w_i^2 x_i^2 y_i^2}}{2\sum_{i=1}^{n} w_i^2 \widetilde{x}_i \widetilde{y}_i} \tag{14}$$

The standard deviation of the major axis (X-axis) and the standard deviation of the minor axis (Y-axis) represent the dispersion of geographic features in the primary and secondary trend directions, respectively. The Equation are (15) and (16) (Huang et al., 2023; Xiang et al., 2026):

$$\sigma_x = \sqrt{\sum_{i=1}^{n} \left(w_i \widetilde{x}_i \cos\theta - w_i \widetilde{y}_i \sin\theta\right)^2 / \sum_{i=1}^{n} w_i^2} \tag{15}$$

$$\sigma_y = \sqrt{\sum_{i=1}^{n} \left(w_i \widetilde{x}_i \sin\theta - w_i \widetilde{y}_i \cos\theta\right)^2 / \sum_{i=1}^{n} w_i^2} \tag{16}$$

3.2.5. Spatial autocorrelation

3.2.5.1. Global Moran's I. Spatial autocorrelation can effectively reveal the spatial clustering patterns, outlier distributions, and spatial spillover effects of variables, providing a preliminary basis for spatial econometric modeling (Ai et al., 2024; Li et al., 2022). To determine whether the degree of synergy exhibits significant spatial autocorrelation across the entire study area, this study calculated the Global Moran's I index.

$$Global\ Moran's\ I = \frac{n\sum_{i=1}^{n}\sum_{j=1}^{n} W_{ij}(x_i - \overline{x})(x_j - \overline{x})}{\sum_{i=1}^{n}\sum_{j=1}^{n} W_{ij}\sum_{i=1}^{n}(x_i - \overline{x})^2} \tag{17}$$

In the formula, n represents the number of spatial units, x_i and x_j represent the observations of units i and, $\overline{x}$ which are the mean values, and W_{ij} represents the spatial weight matrix. Moran's I value is [−1,1], where $I > 0$ indicates positive autocorrelation, $I < 0$ indicates negative autocorrelation, and $I \approx 0$ indicates random distribution (Ai et al., 2024; Wang et al., 2023). Its significance is usually determined by the Z-test (Eq. 18), E(I) represents the mathematical expectation (Ai et al., 2024; Zhang et al., 2025a,c).

$$Z(I) = 1 - E(I) \Big/ \sqrt{E(I^2) - E(I)^2} \tag{18}$$

3.2.5.2. Local Moran's I. Global metrics may mask local heterogeneity, therefore, it is necessary to introduce local spatial autocorrelation methods to identify the clustering patterns of synergy across local space (Liu et al., 2023; Santos et al., 2023):

$$Local\ Moran's\ I = \frac{(x_i - \overline{x})}{\frac{1}{n}\sum_{i=1}^{n}(x_i - \overline{x})^2} \cdot \sum_{j=1}^{n} W_{ij}(x_j - \overline{x}) \tag{19}$$

Local spatial correlation indexes classify spatial relationships into four types (Fig. S3): high-high (HH) (hot spot area), low-low (LL) (cold spot area), high-low (HL) (isolated point where high value is surrounded by low value) and low-high (LH) (depression area where low value is surrounded by high value) (Cui et al., 2022; Qian et al., 2022; Zhang et al., 2023a, 2023b).

3.2.6. GTWR model

Because the influence of spatial heterogeneity is ignored, the parameter estimates obtained by traditional linear regression models are only global averages within the study area, thus masking key information about regional differences (Chen et al., 2025; Guo et al., 2024; Meng et al., 2025). Geographical weighted regression (GWR) models lack consideration of the time factor, ignoring the changes in the effects of different factors at different times (Wang et al., 2024; Yu and Li, 2025). The GTWR model integrates both spatial and temporal coordinates as control variables within the regression framework. This simultaneous incorporation allows the model to effectively handle spatiotemporal nonstationarity and improve the robustness of parameter estimates (Dong et al., 2023; He et al., 2025). This study employs the GTWR model to investigate the associations of various potential influencing factors with the degree of synergy. The basic expression of the GTWR model and the estimation of the regression parameter are as follows (He et al., 2025; Zhang et al., 2025a, 2025b, 2025c):

$$Y_i = \beta_0(u_i, \nu_i, t_i) + \sum_{k=1}^{n} \beta_k(u_i, \nu_i, t_i) X_{ik} + \varepsilon_i, i = 1, 2, \cdots, n. \tag{20}$$

$$\hat{\beta}(u_i, \nu_i, t_i) = \left[X^T W(u_i, \nu_i, t_i) X\right]^{-1} X^T W(u_i, \nu_i, t_i) Y \tag{21}$$

where, Y represents the degree of coordination between EPRCR, and X represents the influencing factors; (u_i, ν_i, t_i)represents the spatiotemporal coordinates of the ith county; $\beta_0(u_i, \nu_i, t_i)$ represents the model constant term ; n is the number of spatial locations; X_{ik}represents the value of the k-th influencing factor in the ith county ; $\beta_k(u_i, \nu_i, t_i)$ represents the regression coefficient of the kth influencing factor in the ith county over time t;ε_i represents the random error term.$W(u_i, \nu_i, t_i) = diag(\alpha_{i1}, \alpha_{i2}, \ldots, \alpha_{in})$ where $\alpha_{ij}$are space-time distance functions of (u_i, ν_i, t_i) corresponding to the weights when adjusting a weighted regression adjacent to city i (Meng et al., 2025; Zhang et al., 2025a, 2025b, 2025c).

In addition, the GTWR model was implemented using the following specifications:

(1) Kernel type: A Gaussian kernel (adaptive) was used to assign spatial and temporal weights. The adaptive kernel adjusts the bandwidth to maintain a consistent number of nearest neighbors across regions with varying observation densities. (2) Bandwidth selection: The optimal bandwidth was determined using the corrected Akaike Information Criterion (AICc) with a golden-section search algorithm, balancing model fit and complexity. (3) Coordinate system: All spatial coordinates were projected to WGS 1984 UTM Zone 48 N (EPSG: 32648) with metric units (meters) for distance calculation. (4) Temporal distance: Temporal distances (years) were scaled to the same range (0–1) as spatial distances using min-max normalization to ensure equal weighting of spatial and temporal dimensions.

3.3. Data sources and processing

3.3.1. Data sources

This study primarily investigates the synergistic effects between EPRCR. Given that atmospheric pollution constitutes Chongqing's most prominent environmental issue, this study primarily analyzes the spatiotemporal variation characteristics of atmospheric pollutants to facilitate a comparison with changes in carbon emissions. The main data involved in this study include air pollutant concentration data, carbon emission data, and related socio-economic data of various districts and counties in Chongqing from 2017 to 2022. The pollutant data primarily comes from the Emissions Database for Global Atmospheric Research (https://edgar.jrc.ec.europa.eu/dataset_ap81) and the China National Environmental Monitoring Center (http://www.cnemc.cn/). In addition, carbon emission data are mainly referenced from the China Carbon Accounting Database (https://ceads.net), Global Carbon Budget Database (https://globalcarbonbudget.org/gcb-2025/), MEIC (http://meicmodel.org.cn/). The nighttime light data was obtained from the DMSP-OLS and NPP-VIIRS satellite products of the National Oceanic and Atmospheric Administration (NOAA). Other indicators, such as population, Gross domestic product (GDP) and urbanization rate, are sourced from the China Environmental Statistics Yearbook, the China County Statistics Yearbook, the Chongqing Statistical Yearbook and the Chongqing Municipal Ecological Environment Status Bulletin. County-level administrative boundary data are from the National Center for Surveying and Mapping, China (http://www.ngcc.cn).

3.3.2. Data processing

To construct the county-level dataset (2017–2022) from multiple sources, we applied the following procedures:

(1) Nighttime-light downscaling: To downscale provincial-level emissions to the county scale, we employed a nighttime-light (NTL) based disaggregation approach using the DMSP/OLS and VIIRS datasets. The downscaling procedure consists of three steps: First, provincial emission totals: Provincial CO_2 emissions were first estimated following IPCC sectoral guidelines (Eggleston et al., 2006). Second, weight calculation: For each county *i* in province p, the allocation weight w_i is computed as Eq. (22):

$$w_i = \frac{NTL_i}{\sum_{j \in p} NTL_i} \tag{22}$$

where NTL_i is the annual sum of DN (Digital Number) values within county *i*. Third, allocation: County-level emissions $E_i = E_p \times w_i$, where E_p is total provincial emission.

(2) Missing data treatment: Missing data imputation affected <25% of county-year observations for any single variable (Table S2). For gaps ≤2 years, we used linear interpolation; for larger gaps, we applied city-level means weighted by county GDP. Counties with >50% missing for core variables were excluded, yielding the final sample of 38 counties.

(3) We also examined the potential impact of data reconstruction on our main conclusions. Comparing the fully imputed dataset (38 counties) to a restricted sample of counties with complete reporting, we found no evidence that the imputation procedures introduced substantial bias into the estimated spatial patterns. These findings suggest that our data reconstruction does not artifactually drive the main spatial conclusions identified in this study.

4. Results and discussion

4.1. Spatiotemporal evolution pattern of carbon and pollutant emissions

4.1.1. Spatiotemporal distribution characteristics of atmospheric pollutants

(1) Temporal variation characteristics of pollutants

As shown in Fig. 2, the main atmospheric pollutants in Chongqing from 2017 to 2022 exhibited different temporal variation trends. In 2017, the annual average concentrations of $PM_{2.5}$ (45 μg/m^3) and O_3 (163 μg/m^3) exceeded the national secondary standards by 0.29 times and 0.63 times, respectively. The annual average concentrations of NO_2 (46 μg/m^3) and PM_{10} (72 μg/m^3) also exceeded the national secondary standard, while the annual average concentrations of SO_2 and CO met the standard. In 2022, the concentrations of major pollutants all decreased, with the annual average concentration of PM_{10} at 48 μg/m^3,

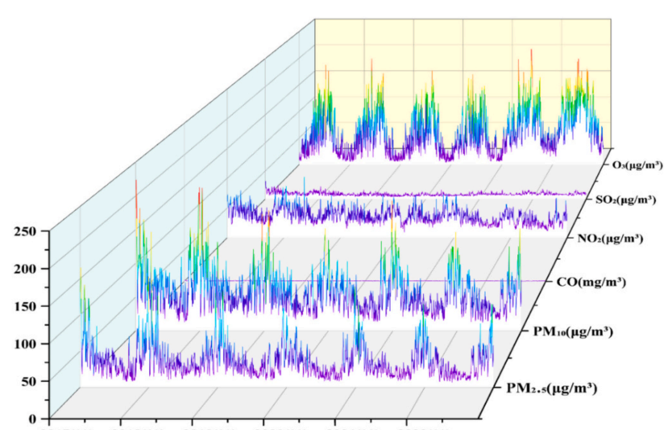

Fig. 2. Air Pollutant Concentrations in Chongqing, 2017–2022.

$PM_{2.5}$ at 31 μg/m^3, NO_2 at 29 μg/m^3, and O_3 at 144 μg/m^3. Overall, Chongqing's air quality improved significantly between 2017 and 2022, with the concentrations of major pollutants generally showing a downward trend. Among them, NO_2 saw the largest decrease (37.0%), while $PM_{2.5}$ decreased by 31.1% and PM_{10} by 33.3%. However, the overall concentrations of major pollutants $PM_{2.5}$, PM_{10} and O_3 still exceed the Class I limits of the Ambient Air Quality Standards and are far from the limits of the WHO 2021 AQGs standards.

The Comprehensive Air Quality Index (CAQI) is a quantitative assessment of the overall air pollution level in a region. The lower the CAQI value, the better the overall annual average air quality in that region (Ye et al., 2018). The CAQI heat map (Fig. S4) further demonstrates that the air quality in various districts and counties of Chongqing gradually improved between 2017 and 2022. In 2017, the CAQI values of most districts and counties were higher than 4.5, indicating that the overall annual average level of air pollutants in these areas was 4.5 times the concentration equivalent of the national secondary standard limit. Furthermore, Qijiang District, Chengkou County, Shizhu County, Xiushan County, Youyang County, and Pengshui County generally had better air quality and smaller fluctuations compared to other districts and counties.

(2) Spatial distribution characteristics of pollutants

In 2017, approximately 85% of districts and counties had $PM_{2.5}$ concentrations exceeding the standard (35 μg/m^3); by 2022, this proportion had dropped significantly to only about 10% (Fig. S5). This indicates that the number of districts and counties meeting the national standard limits of $PM_{2.5}$ gradually increased during the study period. However, the overall $PM_{2.5}$ concentration is still far higher than the WHO, 2021 AQGs annual average limit (5 μg/m^3). As shown in Fig. S6, in 2017, the PM_{10} concentration in all districts and counties of Chongqing exceeded the China I annual average limit (40 μg/m^3), and the concentration in about 40% of the areas was higher than the China II annual average limit (70 μg/m^3). By 2022, the concentration in all districts and counties was lower than the China II annual average limit. NO_2 concentrations also showed a downward trend during the study period. However, in 2017–2018, some areas had concentrations higher than the national annual average limit (40 μg/m^3), mainly located in the main urban area (Fig. S7). Between 2017 and 2022, the annual average concentrations of SO_2 and CO in all districts and counties met the national standard limits (Fig. S8 and S9). Furthermore, during the study period, approximately 90% of the districts and counties had O_3 concentrations exceeding the national limit (100 μg/m^3) (Fig. S10). O_3 concentrations showed a certain downward trend between 2020 and 2021. This may be closely linked to the strict restrictions on personnel movement and traffic implemented during the early stages of the pandemic. Relevant studies have indicated that these measures may lead to atypical shifts in the ratio of the two key precursors (NOx and VOCs) required for ozone formation (Chen et al., 2023a, 2023b, 2023c, 2023d, 2023e, 2023f; Duan et al., 2023). For instance, studies by Duan et al. (2023) and Lin et al. (2022) found that in 2020, strict lockdown measures significantly reduced NOx emissions from traffic sources, thereby potentially inhibiting ozone formation under conditions where VOCs were relatively abundant (Duan et al., 2023; Lin et al., 2022). Furthermore, Pan et al. (2023) and Yan et al. (2024) also pointed out that in 2022, with the resumption of work and production, emissions of NOx and VOCs rebounded rapidly, providing ample "raw materials" for ozone formation (Pan et al., 2023; Yan et al., 2024).

4.1.2. Spatiotemporal distribution characteristics of carbon emissions

Fig. S11 shows the following changes in Chongqing's primary energy consumption structure: coal increased from 53.77% in 2017 to 50.71% in 2022; natural gas increased from 15.00% to 21.87%; clean electricity decreased from 15.6% to 11.54%. Despite this transformation, coal remained the largest share at 50.71% in 2022 (Fig. S11). Carbon emissions from coal consumption accounted for 60.02% of total emissions in 2022. By sector, industry contributed 52.10%, transportation contributed 11.22%, electricity and heat production contributed 30.72% in 2022, with the latter showing an annual growth rate of 10% during 2017–2022. This pattern suggests that coal remains the primary driver of Chongqing's carbon emissions, despite a partial shift toward cleaner energy sources. In addition, as shown in Fig. 3, during the study period, 18 districts/counties (including Jiangjin, Bishan, Yuzhong, Fengjie, and Shizhu) experienced an increase in carbon emissions alongside improved air quality. The remaining districts/counties showed a positive synergy between carbon emission reduction and air quality improvement. This indicates that the level of EPRCR varies across districts/counties.

The standard deviation ellipse and the centroid migration model can intuitively identify the changes in the centroid migration of carbon emissions and the spatial distribution of carbon emission areas (Xiang et al., 2026; Yang et al., 2025). As show in Fig. 4, the dominant spatial distribution of carbon emissions in Chongqing from 2017 to 2022 was southwest-northeast. Overall, the area of the ellipse shows a shrinking trend. This indicates that the spatial clustering effect of carbon emissions is strengthening, with high-emission areas gradually concentrating along this main axis, and regional differentiation becoming increasingly apparent. Furthermore, during the study period, the center of gravity generally exhibited a trend of shifting toward the southeast. The shift in emission intensity was observed from 2017 to 2020 in a southwest direction and from 2020 to 2022 in a northeast direction, reflecting the dynamic changes in the dominant emission areas at different stages. It is worth noting that the center of gravity shifted relatively significantly between 2020 and 2021. This may be due to the uneven pace of industrial recovery in different districts and counties during the post-pandemic economic recovery process, or factors such as the commissioning of certain energy-intensive projects leading to short-term fluctuations in emission patterns.

4.2. Spatiotemporal evolution of the synergy between EPRCR

4.2.1. Temporal variation trend of CCD

Based on the EPRCR analysis framework and referring to existing research results, this study focuses on the synergistic governance of environmental pollution and carbon emissions. A multidimensional evaluation indicator system was constructed—encompassing atmospheric pollution, water pollution, comprehensive environmental quality, and carbon emissions—to comprehensively reflect the synergistic status of regional EPRCR. The entropy weight method was employed to determine the weight coefficients for each indicator (Table 2) (Meng et al., 2025; Nie and Lee, 2023; Zhang et al., 2025a, 2025b, 2025c). The CCD of each district and county from 2017 to 2022 was calculated using the CCD model (Fig. 5). The number of violins on the list from 2017 to 2022 showed an upward trend, indicating that the level of coordinated EPRCR is improving year by year. Besides, the graphs for each year show a clear "clustering" characteristic, meaning that most districts and counties are concentrated in the medium-level coordination range, while a few areas have entered the high-level coordination range. It is noteworthy that some industrial districts, such as Qijiang, Hechuan, and Changshou were located in the low-value anomaly zone, while areas such as Yuzhong, Chengkou, and Youyang were at a relatively high level of coordination. This indicates that the industrial structure has a significant association with the degree of coordination. Examining the boxplot structure, the median steadily increased from 0.56 in 2017 to 0.61 in 2022, indicating a continuous improvement in the city's overall coordination level. Furthermore, the box height showed a narrowing trend, suggesting that the gap between districts and counties is decreasing.

According to the kernel density estimation plot, the center of the main peak of the curve shows a fluctuating trajectory, characterized by first shifting to the right and then slightly shifting to the left (Fig. 6). This

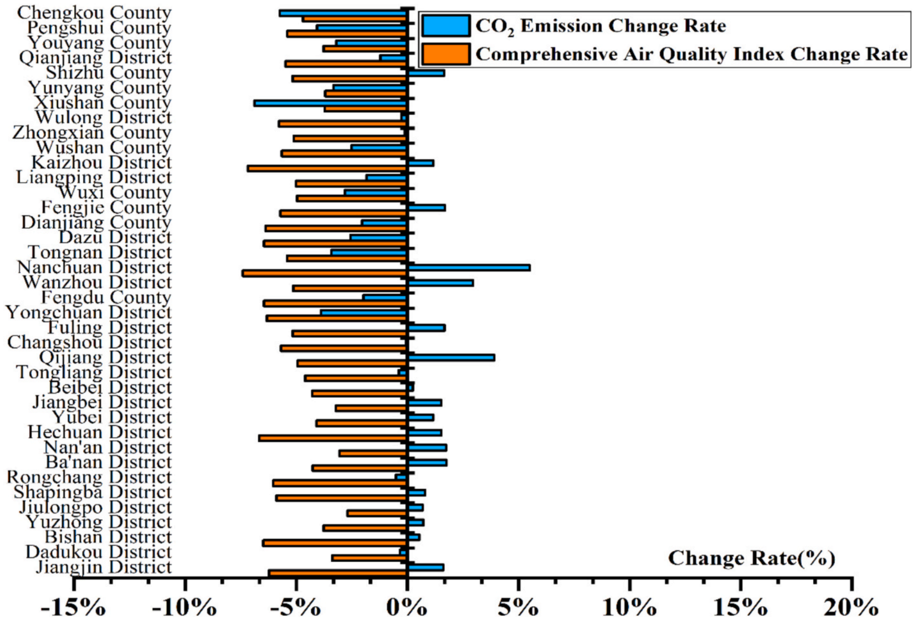

Fig. 3. Change rates of CAQI and CO_2 emissions in various districts and counties of Chongqing, 2017–2022.

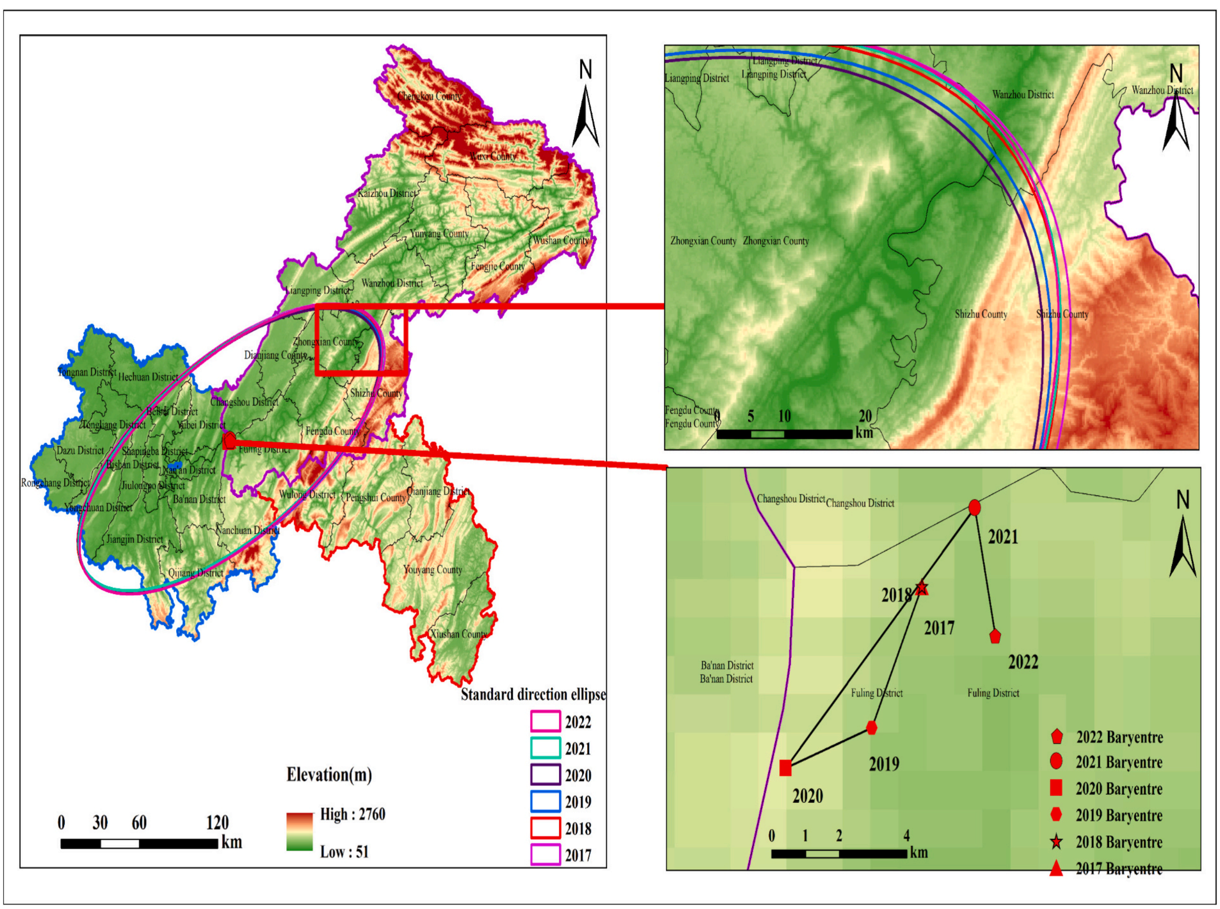

Fig. 4. Center of gravity and standard ellipse of CO_2 emissions.

indicates that, while the overall level of coupling coordination improved during the study period, it remains unstable based on the year-to year fluctuations shown in Fig. 6. The distribution pattern shows that the overall height of the main peak has increased, while its width has decreased. This indicates that the absolute gap between districts and counties is narrowing. Furthermore, the left tail of the curve exhibits a distinct trailing phenomenon, with no significant narrowing observed. This means that traditional industrial areas, represented by Qijiang and Changshou, have long been in a low-coordination range and are at risk of persistently remaining at a low level; while Yuzhong District and

Table 2
Evaluation index system and weights for EPRCR collaboration in districts and counties of chongqing.

Target layer	Criteria layer	Secondary indicator	Tertiary indicators	Unit	Direction	Weight
EPRCR	Environmental pollution reduction system	Intensity of air pollution emissions and treatment	Industrial SO_2 emissions per unit of GDP	$t/10^4$ yuan	−	0.105
			Industrial NOx emissions per unit of GDP	$t/10^4$ yuan	−	0.104
		Intensity of water pollution discharge and treatment	Industrial COD emissions per unit of GDP	$t/10^4$ yuan	−	0.117
			Industrial wastewater discharge per unit of GDP	$10^4t/10^4$ yuan	−	0.070
		Environmental quality improvement status	$PM_{2.5}$ annual average concentration	$\mu g/m^3$	−	0.163
			Proportion of days with good or excellent air quality	%	+	0.041
	Carbon reduction system	Carbon and Energy Efficiency	CO_2 emissions per unit of GDP	$t/10^4$ yuan	−	0.232
			Energy consumption of industrial enterprises above designated size	10^4 tons of standard coal	−	0.095
		Structure and Path	The proportion of the added value of the tertiary industry in GDP	%	+	0.041
			Forest coverage	%	+	0.032

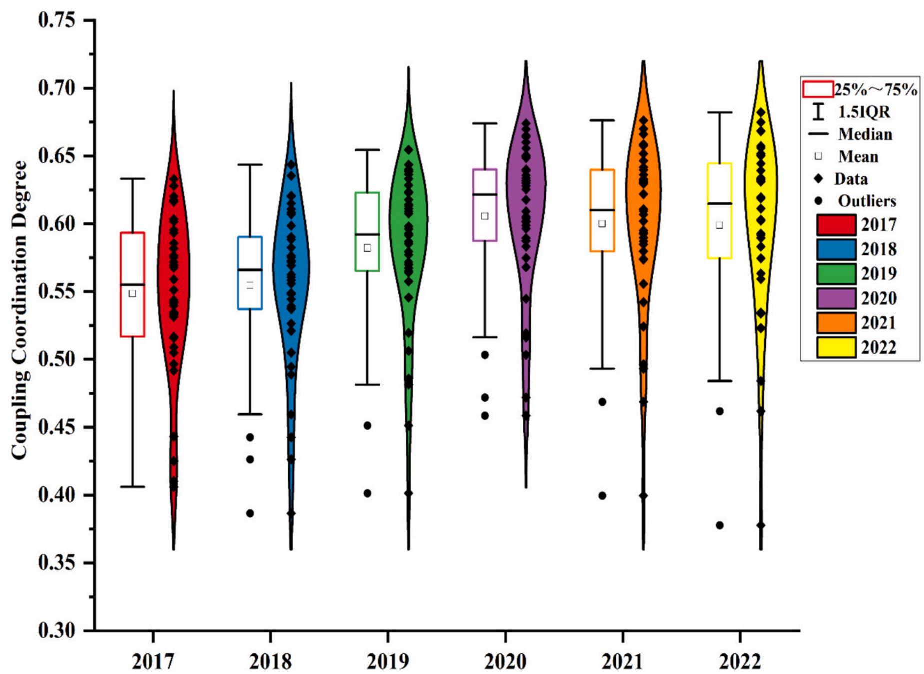

Fig. 5. The trend of CCD.

some ecological conservation areas continue to be in the medium-high value range. The phenomenon of structural persistence suggests that a region's resource endowment and industrial foundation are strongly associated with its initial synergy level. Overall, during the study period, the coupling synergy of most districts and counties was in the range of 0.5–0.7, indicating that most districts and counties were in a range between imbalance and coordinated development during 2017–2022.

4.2.2. Spatial relationship pattern of CCD

Spatial autocorrelation analysis revealed that the global Moran's I value was positive throughout the study period, and generally showed a fluctuating upward trend (Table S3). This indicates that there is a significant positive spatial correlation in the CCD among various districts and counties in Chongqing, and the spatial clustering characteristics are continuously strengthening. Moran's I in 2017 was 0.239 ($Z = 2.45$, $P < 0.05$), indicating that the CCD already showed a certain spatial dependence in the early stage of the study. In 2022, Moran's I rose to 0.278 ($Z = 2.91$, $P < 0.01$), and the degree of clustering was further strengthened. This trend is similar to the findings of related studies on the Chengdu-Chongqing urban agglomeration, namely, the increasing spatial interaction of elements within the region (Guo et al., 2024; Xiang et al., 2025, 2026). Furthermore, Moran's I values for all years during the study period passed the significance test ($P < 0.05$), indicating that the spatial distribution of CCD among districts and counties in Chongqing is not random. This confirms the presence of significant spatial autocorrelation. The radiating or competitive constraints between neighboring regions are associated with spatial dependence and heterogeneity in the CCD.

Furthermore, the local spatial autocorrelation analysis reveals that the hotspots of EPRCR coupling coordination exhibit characteristics of shifting and diffusing from certain areas of the main urban district toward the southeast (Fig. 7). Youyang County was the only region that maintained a high-high agglomeration throughout the entire study period. In addition, the low-low agglomeration areas are mainly concentrated in the strip-shaped areas of southern and western Chongqing, showing a strong spatial persistence. As traditional industrial hubs in Chongqing, Jiangjin District, Qijiang District, and Fuling District consistently fell within the category of "cold spot" areas during the study period. Overall, the spatial pattern of EPRCR in Chongqing during the study period showed characteristics of "large-scale dispersion and small-scale agglomeration." High-value and low-value agglomeration areas exhibited spatial contrast, with coexisting patterns of spatial

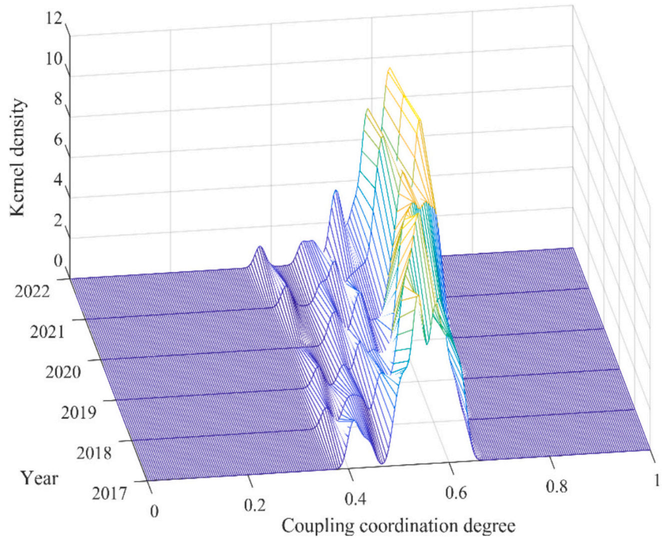

Fig. 6. Kernel density of CCD.

persistence and short-term change over the 2017–2022 period. Hotspots shifted toward the southeastern and northeastern ecological hinterlands and coldspots persisted in the industrial belt surrounding the main urban area (Fig. 7).

4.2.3. Sensitivity analysis of subsystem weights in CCD

To test the robustness of the CCD results to the equal-weight assumption ($\alpha = \beta = 0.5$), we additionally calculated the CCD index under alternative weight scenarios: (i) pollution-weighted ($\alpha = 0.6$, $\beta = 0.4$); (ii) carbon-weighted ($\alpha = 0.4$, $\beta = 0.6$). Spearman's rank correlation coefficients were calculated between the CCD rankings derived from the equal-weight baseline and each alternative scheme.

The results are summarized in Table S4. Sensitivity analysis of alternative weighting schemes revealed that the Spearman rank correlation coefficients between the CCD values under the equal-weight baseline scheme and their counterparts under the pollution-weighted scheme ($\rho = 0.993$, $p < 0.01$) and the carbon-weighted scheme ($\rho = 0.995$, $p < 0.01$) both exceed 0.99, indicating that their ranking results are nearly identical. Furthermore, we quantitatively assessed the consistency of spatial clustering by calculating the retention rate of spatial clustering types (High-High, Low-Low, High-Low, and Low-High) for each county-level unit under alternative weighting schemes. The results (Table S4) indicate that, under both alternative weighting schemes, over 96% of the county-level units retained the same spatial clustering type as in the benchmark equal-weighting scheme, demonstrating that the spatial clustering patterns did not undergo any substantial changes.

4.3. Spatiotemporal heterogeneity of varying associations for EPRCR

4.3.1. Model specification and optimization test

Considering data availability and rationality, this study selected six specific explanatory variables from four dimensions: socio-economic development level, regional industrial structure, energy consumption level, and technological innovation. These variables were used to reveal the coordinated spatiotemporal evolution characteristics of EPRCR across various districts and counties of Chongqing (Table S5). Descriptive statistical analysis revealed significant differences in the variables affecting the coordinated promotion of EPRCR across different districts and counties, indicating a certain spatial effect on the degree of coordination in EPRCR (Table S6). In addition, the variance inflation factor (VIF) of each influencing factor was calculated using STATA software. The results showed that the VIF values of all variables were less than 10

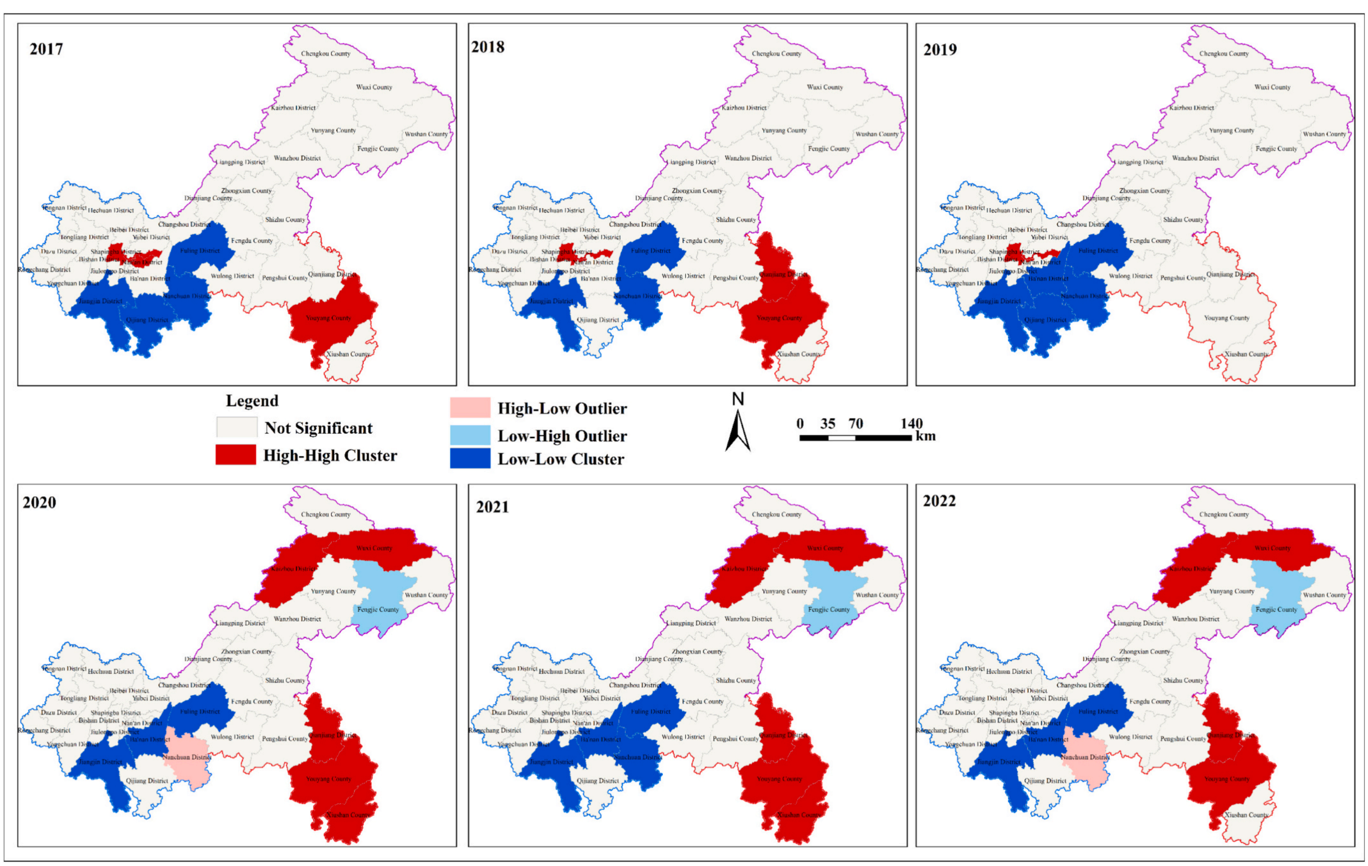

Fig. 7. Spatial clustering analysis of CCD.

(Table 3). This indicates that there is no significant multicollinearity among the explanatory variables.

Residual spatial autocorrelation was assessed using Moran's I. As shown in Table 4, GTWR effectively reduced residual spatial autocorrelation compared to OLS and GWR (Moran's $I = 0.0034$, $p > 0.05$), indicating that the model captures most of the spatial dependence. Table 4 also presents the fit statistics for OLS, GWR, and GTWR models. The OLS model yielded an R^2 of 0.56 and an AICc of 474.96. The GWR model showed modest improvement ($R^2 = 0.57$, $\Delta R^2 = +0.01$; AICc = 473.96). The GTWR model, which incorporates both spatial and temporal non-stationarity, achieved substantially better fit ($R^2 = 0.67$, $\Delta R^2 = +0.10$ relative to GWR; AICc = 461.21). The notable improvement from GWR to GTWR ($\Delta R^2 = 0.10$) indicates that the relationships between explanatory variables and the synergy index are not only spatially varying but also temporally evolving over the 2017–2022 period. This means that GWR, which assumes temporally stationary coefficients, misses important time-varying dynamics. The improvement is both statistically meaningful (lower AICc, lower residual spatial autocorrelation) and substantively meaningful, as it reveals time-dependent patterns that are critical for policy timing and targeting. Therefore, this study employs the GTWR model for analysis.

Table 4
Comparison of model fit superiority.

Model	R^2	ΔR^2	Adj-R2	RSS	AICc	Residual Moran's I
OLSR	0.56	–	0.55	100.36	474.96	−0.0102
GWR	0.57	+0.01	0.56	97.41	473.96	−0.0054
GTWR	0.67	+0.10	0.66	75.07	461.21	0.0034

4.3.2. *GTWR model regression result analysis*

The quantitative evaluation results of the GTWR model show that the regression coefficients of each influencing factor have both positive and negative values, indicating that there is significant spatial heterogeneity among the factors (Table S7). Per capita GDP and patent counts are positively associated with EPRCR, while population density, secondary sector share, and industrial energy consumption show negative associations. The urbanization rate has the weakest association. Industrial energy consumption shows a more pronounced negative association with EPRCR than other factors. Population density shows a persistent negative association with EPRCR throughout the study period. Spatially, the magnitude of this negative association varies across districts, with densely populated urban cores exhibiting a stronger effect than peri-urban areas.

In terms of industrial structure, the regression coefficient for the share of value added by the secondary sector is negative, indicating a negative association with EPRCR. In Southeast Chongqing, the negative coefficient is larger in magnitude, while in Northeast Chongqing, it is relatively smaller (Fig. 8). For technological innovation, core urban districts show high-value coefficients, while Northeast Chongqing shows isolated high-value clusters (Fig. 8). In Southeast Chongqing and Wushan, patent coefficients are not statistically significant.

5. Conclusion

5.1. *Summary of findings*

This study comprehensively employs a variety of spatial statistical and econometric models to systematically reveal—from the perspective of districts and counties—the spatiotemporal heterogeneity, coupled nature of synergistic reduction, and spatiotemporally varying associations of environmental pollutants and carbon emissions in Chongqing during the period of 2017–2022. The main findings are as follows:

(1) From 2017 to 2022, major atmospheric pollutants in Chongqing showed a significant downward trend, but concentrations remained above the WHO 2021 AQGs limits. Centroid-Standard Deviational Ellipse analysis reveals a strengthening spatial agglomeration of carbon emissions, with the centroid oscillating along a southwest-northeast axis. This spatial structure persisted throughout the study period, indicating that high-carbon industries remained concentrated in certain districts without significant spatial diffusion.

(2) Kernel density estimation and spatial autocorrelation analysis indicate that the CCD of EPRCR increased overall from 2017 to 2022, with periodic year-to-year variations. Hot spots of CCD shifted toward the southeastern and northeastern districts-areas with lower industrial density—while cold spots remained concentrated in the industrial belt surrounding the main urban area.

(3) The GTWR model shows that the direction and magnitude of association between each influencing factor and EPRCR synergy varied across space and time. Per capita GDP and technological innovation show the strongest positive associations with the synergy of EPRCR, while energy consumption by large industrial enterprises exhibits the strongest negative association. The positive association of per capita GDP was largest in the main urban metropolitan area and smaller in Northeast and Southeast Chongqing. The association of technological innovation remained stable in its spatial pattern throughout the study period.

5.2. *Policy implications*

As a typical mountainous city, Chongqing exhibits significant spatial heterogeneity in EPRCR synergy across its main urban area, suburban districts, northeastern counties, and southeastern counties. A uniform emission reduction strategy is therefore unlikely to be effective. Based on the findings for Chongqing (2017–2022), the following policy recommendations are intended to inform local efforts toward carbon peaking and neutrality targets.

(1) The finding that high-carbon industries remained concentrated in certain districts without significant spatial diffusion suggests that market forces or existing policies have not incentivized relocation. The following measures are recommended: First, impose binding emission caps on the districts where the centroid has concentrated. Second, establish inter-district fiscal transfers to compensate these districts for accelerated decarbonization. Finally, use centroid oscillation as a lead indicator: lack of diffusion within two years triggers automatic escalation of local reduction targets.

(2) Spatial autocorrelation analysis shows positive spatial spillover effects of EPRCR synergy. The following measures are recommended to enhance these effects: First, construct a multi-level spatial collaborative governance system linking the main urban area, industrial belt, and peripheral districts. Second, use the

Table 3
Covariance test results.

Explained variable	Population density	Urbanization rate	Per capita GDP	Proportion of secondary industry	Energy consumption of industrial enterprises above designated size	Number of patents granted
Tolerance	0.246	0.285	0.284	0.581	0.749	0.408
VIF	4.067	3.512	3.518	1.720	1.335	2.451

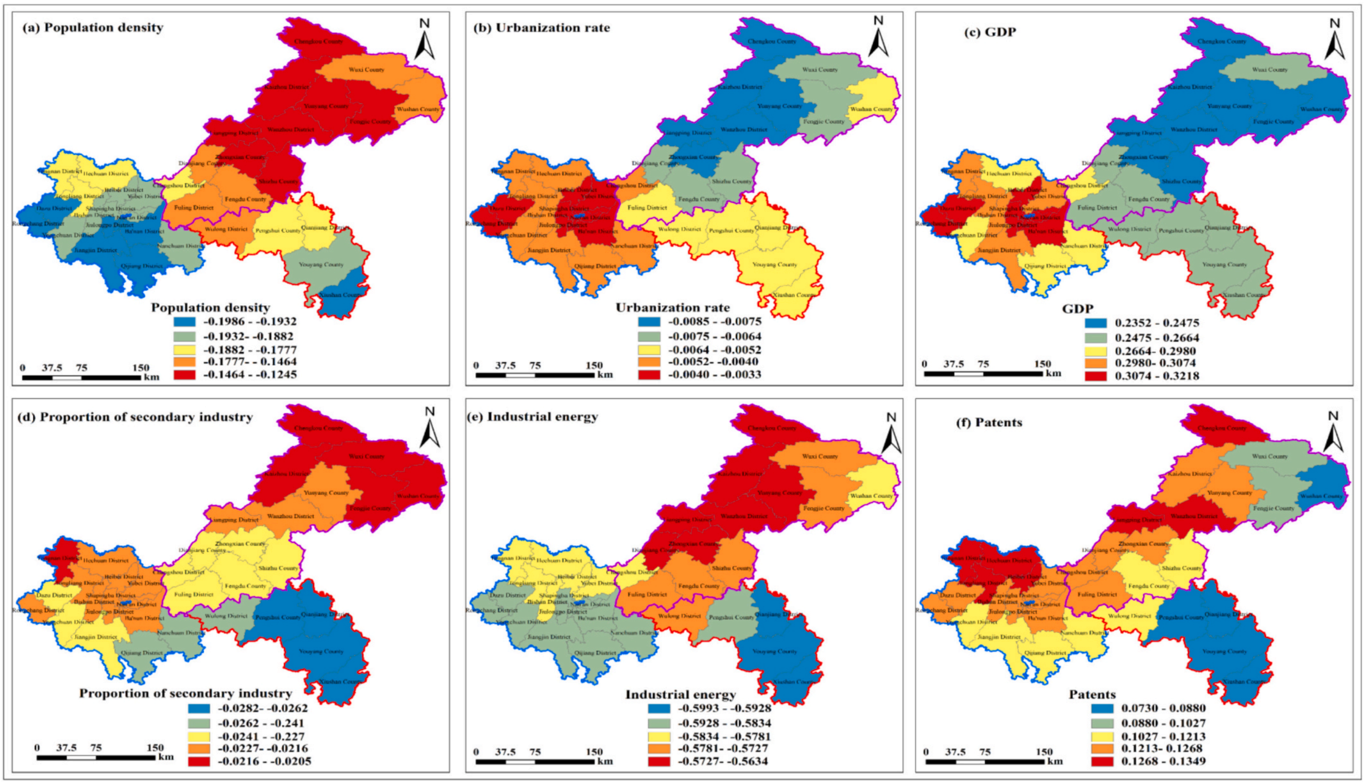

Fig. 8. The spatial heterogeneity of influencing factors in the CCD of EPRCR.

main urban area's established capacity in green technology, green finance, and environmental regulation as a hub. Establish formal mechanisms (e.g., inter-district technology transfer agreements, joint environmental investment funds) to transmit best practices to surrounding areas with lower CCD values.

(3) The GTWR results show that energy consumption by large industrial enterprises has a persistent negative association with EPRCR synergy. The following technology-focused measures are recommended: First, in cold spot areas (industrial belt), set energy intensity reduction targets 10–15% higher than the city average and implement facility-level energy audits for large industrial consumers. Second, in the main urban area, prioritize public R&D funding for green and low-carbon technologies, with defined milestones for commercialization. Third, in Southeast Chongqing (mining and metallurgy cluster), deploy deep mineral processing technologies and solid waste valorization systems, linking technology transfer to verifiable emission reductions. Finally, in northeastern Chongqing (an ecologically sensitive zone), efforts focus on technologies for non-point source pollution control and ecological restoration, alongside an evaluation of the effectiveness of pilot initiatives.

5.3. Limitations and future research

Although this study provides new evidence for revealing the spatiotemporally varying associations of synergistic EPRCR, it still has certain limitations and requires further investigation in the future:

First, this study has limitations in terms of data scale and precision. The analysis is primarily conducted at the district-county administrative unit. However, production activities at the micro-enterprise level and pollutant transport processes at the urban agglomeration scale may obscure more refined spatiotemporal dynamic associations. Furthermore, this study only captures short-term spatial persistence and recent trends; rigorous testing of long-term phenomena would require longer time-series data. Therefore, future research could attempt to integrate satellite-retrieved remote sensing data with enterprise-level pollution monitoring databases and conduct multi-scale nested analyses over longer time spans to further improve the accuracy of the findings.

Secondly, the indicator system lacks completeness. When constructing the evaluation system for the coupling coordination of EPRCR, emission intensity was the primary consideration. However, ecological and social dimensions—such as environmental carrying capacity and health benefits—were not fully incorporated. Furthermore, the environmental pollution reduction system did not take into account indicators such as soil pollution and solid waste. Future research should further refine the evaluation framework for environmental pollution reduction systems. In addition, the value of ecosystem services or public health exposure risks could be incorporated into this framework, thereby constructing a more comprehensive assessment model for the "natural–social–economic" complex system.

Finally, the depth of the analysis regarding the spatiotemporally varying associations of potential influencing factors remains to be further explored. The GTWR method only captures statistical associations and spatiotemporal nonstationarity in the relationship between explanatory variables and the coordination index. While such spatially and temporally varying coefficients may suggest potential influencing factors, they do not constitute evidence of causal mechanisms. Future work should combine GTWR with quasi-experimental designs (e.g., difference-in-differences, instrumental variables, or panel Granger causality) to more rigorously identify causal relationships.

CRediT authorship contribution statement

Xiaoju Li: Writing – original draft, Software, Methodology, Investigation, Formal analysis, Data curation. **Luqman Chuah Abdullah:** Writing – review & editing, Supervision. **Lichao Nengzi:** Writing – review & editing. **Jinzhao Hu:** Writing – review & editing. **Shafreeza Sobri:** Writing – review & editing. **Mohamad Syazarudin Md Said:**

Writing – review & editing. **Siti Aslina Hussain:** Writing – review & editing. **Tan Poh Aun:** Writing – review & editing.

Consent to participate

Not applicable.

Consent to publish

Not applicable.

Ethics approval

Not applicable. My manuscript does not report on or involve the use of any animal or human data or tissue.

Funding

This work was supported by the National Natural Science Foundation, China [grant numbers: 41967033]; Sichuan Province Outstanding Youth Fund Project [grant numbers: 13QNJJ0110]; Sichuan Provincial Department of Education Innovation Team Project [grant numbers: 14TD0020]; the Project of Sichuan Meteorological Disaster Forecasting, Early Warning and Emergency Management Research Center, Sichuan Province, China [grant numbers: ZHYJ21-YB08, ZHYJ24-YB02]; Sichuan Provincial Philosophy and Social Sciences Planning Project "Construction of Beautiful Sichuan" [grant numbers:SC25ST016]; Sichuan Higher Education Social Science Key Research Base Chengdu-Chongqing Economic Circle Science and Technology Innovation and New Economy Research Center Project [grant numbers: CYCX2024ZC23]; Open Fund Project of Sichuan Mineral Resources Research Center, China [grant numbers: SCKCZY2025-ZC004]; Chengdu Research Center for Integrating into the New Pattern of Dual Circulation Development and Sichuan Research Center for Integrating into the New Pattern of Dual Circulation Development [grant numbers: SXH202514].

Declaration of competing interest

The authors declare that they have no known competing financial interests or personal relationships that could have appeared to influence the work reported in this paper.

Acknowledgements

The authors would like to acknowledge to Xichang University, Sichuan Province, China and Department of Chemical and Environmental Engineering, Universiti Putra Malaysia for assistance and helpful with supporting to the writing of this article.

Appendix A. Supplementary data

Supplementary data to this article can be found online at https://doi.org/10.1016/j.ecolind.2026.115099.

Data availability

Data openly available in a public repository.

References

Ai, M., Chen, X., Yu, Q., 2024. Spatial correlation analysis between human disturbance intensity (HDI) and ecosystem services value (ESV) in the Chengdu-Chongqing urban agglomeration. Ecol. Indic. 158 (January), 111555. https://doi.org/10.1016/j.ecolind.2024.111555.

Cao, W., Yuan, X., 2019. Region-county characteristic of spatial-temporal evolution and influencing factor on land use-related CO2 emissions in Chongqing of China, 1997–2015. J. Clean. Prod. 231, 619–632. https://doi.org/10.1016/j.jclepro.2019.05.248.

Chen, L., Wang, D., Shi, R., 2022. Can China ' s Carbon Emissions Trading System Achieve the Synergistic Effect of Carbon Reduction and Pollution Control ?.

Chen, S., Tan, Z., Mu, S., Wang, J., Chen, Y., He, X., 2023a. Synergy level of pollution and carbon reduction in the Yangtze River Economic Belt : Spatial-temporal evolution characteristics and driving factors. Sustain. Cities Soc. 98 (174), 104859. https://doi.org/10.1016/j.scs.2023.104859.

Chen, S., Tan, Z., Wang, J., Zhang, L., He, X., Mu, S., 2023b. Spatial and temporal evolution of synergizing the reduction of pollution and carbon emissions and examination on comprehensive pilot effects – evidence from the national eco-industrial demonstration parks in China. Environ. Impact Assess. Rev. 101 (174).

Chen, X., Di, Q., Jia, W., Hou, Z., 2023c. Spatial correlation network of pollution and carbon emission reductions coupled with high-quality economic development in three Chinese urban agglomerations. Sustain. Cities Soc. 94 (November 2022), 104552. https://doi.org/10.1016/j.scs.2023.104552.

Chen, X., Meng, Q., Wang, K., Liu, Y., Shen, W., 2023d. Spatial patterns and evolution trend of coupling coordination of pollution reduction and carbon reduction along the Yellow River Basin. China. Ecological Indicators 154 (April), 110797. https://doi.org/10.1016/j.ecolind.2023.110797.

Chen, Y., Wang, M., Yao, Y., Zeng, C., Zhang, W., Yan, H., Gao, P., Fan, L., Ye, D., 2023e. Research on the ozone formation sensitivity indicator of four urban agglomerations of China using Ozone Monitoring Instrument (OMI) satellite data and ground-based measurements. Sci. Total Environ. 869 (January), 161679. https://doi.org/10.1016/j.scitotenv.2023.161679.

Chen, Y., Zhao, Z., Yi, W., Hong, J., Zhang, B., 2023f. Has China achieved synergistic reduction of carbon emissions and air pollution? Evidence from 283 Chinese cities. Environ. Impact Assess. Rev. 103 (August), 107277. https://doi.org/10.1016/j.eiar.2023.107277.

Chen, L., Li, X., Kang, X., Liu, W., Wang, M., 2024. Analysis of the cooperative development of multiple systems for urban Economy-Energy-Carbon: A case study of Chengdu-Chongqing Economic Circle. Sustain. Cities Soc. 108 (December 2023), 105395. https://doi.org/10.1016/j.scs.2024.105395.

Chen, M., You, D., Chen, Z., Dai, F., 2025. Synergistic and divergent effects of block morphology on carbon emissions and PM 2 . 5 pollution in Wuhan, China. Sustain. Cities Soc. 134 (September), 106889. https://doi.org/10.1016/j.scs.2025.106889.

China Media Research Institute, 2024. China Energy Big Data Report (2024) https://www.baogaoting.com/info/632991.

Cui, Y., Khan, S.U., Deng, Y., Zhao, M., 2022. Spatiotemporal heterogeneity, convergence and its impact factors: perspective of carbon emission intensity and carbon emission per capita considering carbon sink effect. Environ. Impact Assess. Rev. 92 (March 2021), 106699. https://doi.org/10.1016/j.eiar.2021.106699.

Cui, Q., Liu, Y., Ali, T., Gao, J., Chen, H., 2020. Economic and climate impacts of reducing China's renewable electricity curtailment: A comparison between CGE models with alternative nesting structures of electricity. Energy Econ. 91, 104892. https://doi.org/10.1016/j.eneco.2020.104892.

Cui, H., Lu, Y., Zhou, Y., He, G., Li, Q., Liu, C., Wang, R., Du, D., Song, S., Cheng, Y., 2022a. Spatial variation and driving mechanism of polycyclic aromatic hydrocarbons (PAHs) emissions from vehicles in China. J. Clean. Prod. 336 (August 2021). https://doi.org/10.1016/j.jclepro.2021.130210.

Cui, Z., Fu, X., Wang, J., Qiang, Y., Jiang, Y., Long, Z., 2022b. How does COVID-19 pandemic impact cities' logistics performance? An evidence from China's highway freight transport. Transp. Policy 120 (February), 11–22. https://doi.org/10.1016/j.tranpol.2022.03.002.

Deng, C., Qin, C., Li, Z., Li, K., 2022. Spatiotemporal variations of PM2.5 pollution and its dynamic relationships with meteorological conditions in Beijing-Tianjin-Hebei region. Chemosphere 301 (February), 1–9. https://doi.org/10.1016/j.chemosphere.2022.134640.

Dong, H., Yang, J., 2024. Study on regional carbon quota allocation at provincial level in China from the perspective of carbon peak. J. Environ. Manag. 351 (November 2023), 119720. https://doi.org/10.1016/j.jenvman.2023.119720.

Dong, Z., Xia, C., Fang, K., Zhang, W., 2022. Effect of the carbon emissions trading policy on the co-benefits of carbon emissions reduction and air pollution control. Energy Policy 165 (April), 112998. https://doi.org/10.1016/j.enpol.2022.112998.

Dong, F., Li, J., Huang, J., Lu, Y., Qin, C., Zhang, X., Lu, B., Liu, Y., Hua, Y., 2023. A reverse distribution between synergistic effect and economic development: An analysis from industrial SO_2 decoupling and CO_2 decoupling. Environ. Impact Assess. Rev. 99 (July 2022), 107037. https://doi.org/10.1016/j.eiar.2023.107037.

Duan, X., Yan, Y., Xie, K., Niu, Y., Xu, Y., Peng, L., 2023. Impact of primary emission variations on secondary inorganic aerosol formation: Prospective from COVID-19 lockdown in a typical northern China city. Environ. Pollut. 323 (November 2022), 121355. https://doi.org/10.1016/j.envpol.2023.121355.

Duan, Z., Wei, T., Xie, P., Lu, Y., 2024. Co-benefits and influencing factors exploration of air pollution and carbon reduction in China: based on marginal abatement costs. Environ. Res. 252 (P1), 118742. https://doi.org/10.1016/j.envres.2024.118742.

Eggleston, H.S., Buendia, L., Miwa, K., Ngara, T., 2006. 2006. Tanabe. In: IPCC Guidelines for National Greenhouse Gas Inventories. Prepared by the National Greenhouse Gas Inventories Programme. IGES, Japan.

Fang, J., Yang, Y., Zou, X., Xu, H., Wang, S., Wu, R., Jia, J., Xie, Y., Yang, H., Yuan, N., Hu, M., Deng, Y., Zhao, Y., Wang, T., Zhu, Y., Ma, X., Fan, M., Wu, J., Song, X., Huang, W., 2022. Maternal exposures to fine and ultrafine particles and the risk of preterm birth from a retrospective study in Beijing, China. Sci. Total Environ. 812 (38). https://doi.org/10.1016/j.scitotenv.2021.151488.

Feng, X., Zhang, X., Wang, J., 2023. Update of SO2 emission inventory in the megacity of Chongqing, China by inverse modeling. Atmos. Environ. 294 (October 2022), 119519. https://doi.org/10.1016/j.atmosenv.2022.119519.

Guo, Y., Chen, B., Li, Y., Zhou, S., Zou, X., Zhang, N., Zhou, Y., Chen, H., Zou, J., Zeng, X., Shan, Y., Li, J., 2022. The co-benefits of clean air and low-carbon policies on heavy metal emission reductions from coal-fired power plants in China. Resour. Conserv. Recycl. 181 (February), 106258. https://doi.org/10.1016/j.resconrec.2022.106258.

Guo, M., Hamm, N.A.S., Chen, B., 2024. Understanding air pollution reduction from the perspective of synergy with carbon mitigation in China from 2008 to 2017. J. Environ. Manag. 367 (June), 122017. https://doi.org/10.1016/j.jenvman.2024.122017.

Haddad, P., Kutlar Joss, M., Weuve, J., Vienneau, D., Atkinson, R., Brook, J., Chang, H., Forastiere, F., Hoek, G., Kappeler, R., Lurmann, F., Sagiv, S., Samoli, E., Smargiassi, A., Szpiro, A., Patton, A.P., Boogaard, H., Hoffmann, B., 2023. Long-term exposure to traffic-related air pollution and stroke: a systematic review and meta-analysis. Int. J. Hyg. Environ. Health 247 (November 2022), 114079. https://doi.org/10.1016/j.ijheh.2022.114079.

Han, X., He, X., Xiong, W., Shi, W., 2023. Effects of urbanization on CO2 emissions, water use and the carbon-water coupling in a typical dual-core urban agglomeration in China. Urban Clim. 49 (December 2022), 101572. https://doi.org/10.1016/j.uclim.2023.101572.

Harper, A., Baker, P.N., Xia, Y., Kuang, T., Zhang, H., Chen, Y., Han, T.L., Gulliver, J., 2021. Development of spatiotemporal land use regression models for PM2.5 and NO2 in Chongqing, China, and exposure assessment for the CLIMB study. Atmos. Pollut. Res. 12 (7), 101096. https://doi.org/10.1016/j.apr.2021.101096.

He, C., Wang, Y., Zhang, Z., Zhang, P., Wu, Q., 2025. Spatial heterogeneity in air pollution-carbon synergies: global evidence of decoupled development and disordered coordination. Ecol. Indic. 181 (August), 114473. https://doi.org/10.1016/j.ecolind.2025.114473.

Huang, Z., Jia, H., Shi, X., Xie, Z., Cheng, J., 2023. Revealing the impact of China's clean air policies on synergetic control of CO_2 and air pollutant emissions: evidence from Chinese cities. J. Environ. Manag. 344 (June), 118373. https://doi.org/10.1016/j.jenvman.2023.118373.

Huo, T., Cao, R., Xia, N., Hu, X., Cai, W., Liu, B., 2022. Spatial correlation network structure of China's building carbon emissions and its driving factors: a social network analysis method. J. Environ. Manag. 320 (August), 115808. https://doi.org/10.1016/j.jenvman.2022.115808.

Huynh, C.M., Le, Q.N., Huong, T., Lam, T., 2023. Is air pollution a government failure or a market failure? Global evidence from a multi-dimensional analysis. Energy Policy 173 (December 2022), 113384. https://doi.org/10.1016/j.enpol.2022.113384.

Ji, S., Zhang, Z., Meng, F., Luo, H., Yang, M., Wang, D., Tan, Q., Deng, Y., Gong, Z., 2024. Scenario simulation and synergistic effect analysis of CO_2 and atmospheric pollutant emission reduction in urban transport sector: a case study of Chengdu, China. J. Clean. Prod. 438 (January), 140841. https://doi.org/10.1016/j.jclepro.2024.140841.

Jia, W., Li, L., Lei, Y., Wu, S., 2023a. Synergistic effect of CO_2 and $PM_{2.5}$ emissions from coal consumption and the impacts on health effects. J. Environ. Manag. 325 (October 2022). https://doi.org/10.1016/j.jenvman.2022.116535.

Jia, W., Li, L., Lei, Y., Wu, S., 2023b. Synergistic effect of CO_2 and $PM_{2.5}$ emissions from coal consumption and the impacts on health effects. J. Environ. Manag. 325 (September 2022). https://doi.org/10.1016/j.jenvman.2022.116535.

Jia, W., Li, L., Zhu, L., Lei, Y., Wu, S., Dong, Z., 2024. The synergistic effects of $PM_{2.5}$ and CO_2 from China's energy consumption. Sci. Total Environ. 908 (October 2023). https://doi.org/10.1016/j.scitotenv.2023.168121.

Lei, X., Liu, H., Li, S., Luo, Q., Cheng, S., Hu, G., Wang, X., Bai, W., 2024. Coupling coordination analysis of urbanization and ecological environment in Chengdu-Chongqing urban agglomeration. Ecol. Indic. 161 (December 2023), 111969. https://doi.org/10.1016/j.ecolind.2024.111969.

Li, L., Mi, Y., Lei, Y., Wu, S., Li, L., Hua, E., Yang, J., 2022. The spatial differences of the synergy between CO2 and air pollutant emissions in China's 296 cities. Sci. Total Environ. 846 (February). https://doi.org/10.1016/j.scitotenv.2022.157323.

Lin, C., Song, Y., Louie, P.K.K., Yuan, Z., Li, Y., Tao, M., Li, C., Fung, J.C.H., Ning, Z., Lau, A.K.H., Lao, X.Q., 2022. Risk tradeoffs between nitrogen dioxide and ozone pollution during the COVID-19 lockdowns in the Greater Bay area of China. Atmosph. Pollut. Res. 13 (10), 101549. https://doi.org/10.1016/j.apr.2022.101549.

Liu, H., Liu, J., Li, M., Gou, P., Cheng, Y., 2022a. Assessing the evolution of PM2.5 and related health impacts resulting from air quality policies in China. Environ. Impact Assess. Rev. 93 (December 2021), 106727. https://doi.org/10.1016/j.eiar.2021.106727.

Liu, Y., Tian, J., Zheng, W., Yin, L., 2022b. Spatial and temporal distribution characteristics of haze and pollution particles in China based on spatial statistics. Urban Clim. 41 (November 2021), 101031. https://doi.org/10.1016/j.uclim.2021.101031.

Liu, X., Qin, C., Liu, B., Ahmed, A.D., Ding, C.J., Huang, Y., 2023. The economic and environmental dividends of the digital development strategy: evidence from Chinese cities. J. Clean. Prod. 440 (December 2023), 140398. https://doi.org/10.1016/j.jclepro.2023.140398.

Liu, K., Ren, G., Dong, S., Xue, Y., 2024. The synergy between pollution reduction and carbon reduction in Chinese cities and its influencing factors. Sustain. Cities Soc. 106 (October 2023), 105348. https://doi.org/10.1016/j.scs.2024.105348.

Long, J., Dai, C., Kuang, S., Zhao, H., Liu, D., Luo, Q., Wang, K., 2022. A switching dynamic model based on phased COVID-19 data in Chongqing and its evaluation. Infect. Genet. Evol. 100 (March), 105270. https://doi.org/10.1016/j.meegid.2022.105270.

Lu, H., Xie, M., Liu, X., Liu, B., Liu, C., Zhao, X., Du, Q., Wu, Z., Gao, Y., Xu, L., 2022. Spatial-temporal characteristics of particulate matters and different formation mechanisms of four typical haze cases in a mountain city. Atmos. Environ. 269 (November 2021), 118868. https://doi.org/10.1016/j.atmosenv.2021.118868.

Meng, Q., Chen, X., Wang, H., Shen, W., Duan, P., Liu, X., 2025. Spatiotemporal evolution and driving factors of the synergistic effects of pollution control and carbon reduction in China. Ecol. Indic. 170, 113103. https://doi.org/10.1016/j.ecolind.2025.113103.

Nie, C., Lee, C., 2023. Synergy of pollution control and carbon reduction in China: spatial – temporal characteristics, regional differences, and convergence. Environ. Impact Assess. Rev. 101 (April), 107110. https://doi.org/10.1016/j.eiar.2023.107110.

Pan, W., Gong, S., Lu, K., Zhang, L., Xie, S., Liu, Y., Ke, H., Zhang, X., Zhang, Y., 2023. Multi-scale analysis of the impacts of meteorology and emissions on PM2.5 and O3 trends at various regions in China from 2013 to 2020 3. Mechanism assessment of O3 trends by a model. Sci. Total Environ. 857 (October 2022), 159592. https://doi.org/10.1016/j.scitotenv.2022.159592.

Qian, H., Xu, S., Cao, J., Ren, F., Wei, W., Meng, J., 2021. Air pollution reduction and climate co-benefits in China's industries. Nat. Sustainability 4 (May). https://doi.org/10.1038/s41893-020-00669-0.

Qian, Y., Wang, H., Wu, J., 2022. Spatiotemporal association of carbon dioxide emissions in China's urban agglomerations. J. Environ. Manage. 323 (August), 116109. https://doi.org/10.1016/j.jenvman.2022.116109.

Qin, P., Ren, C., Li, L., Lei, Y., Wu, S., 2023. Evaluation of PM2.5 and CO2 synergistic emission reduction and its driving factors in China. J. Clean. Prod. 428 (September).

Ren, Y., Shao, Y., Xia, J., Liu, A., Lei, S., 2025. Synergistic optimization between green and low-carbon energy transition and reduction of pollution and carbon emissions in the Chengdu-Chongqing economic Circle: based on spatiotemporal evolution and spatial heterogeneity analysis. Energy 339 (October), 139005. https://doi.org/10.1016/j.energy.2025.139005.

Roswall, N., Poulsen, A.H., Hvidtfeldt, U.A., Hendriksen, P.F., Boll, K., Halkjær, J., Ketzel, M., Brandt, J., Frohn, L.M., Christensen, J.H., Im, U., Sørensen, M., Raaschou-Nielsen, O., 2023. Exposure to ambient air pollution and lipid levels and blood pressure in an adult, Danish cohort. Environ. Res. 220 (December 2022). https://doi.org/10.1016/j.envres.2022.115179.

Santos, V.S., Siqueira, T.S., Silva, J.R.S., Gurgel, R.Q., 2023. Spatial clustering of low rates of COVID-19 vaccination among children and adolescents and their relationship with social determinants of health in Brazil: a nationwide population-based ecological study. Public Health 214, 38–41. https://doi.org/10.1016/j.puhe.2022.10.024.

Shao, S., Cheng, S., Jia, R., 2023. Can low carbon policies achieve collaborative governance of air pollution? Evidence from China's carbon emissions trading scheme pilot policy. Environ. Impact Assess. Rev. 103 (July), 107286. https://doi.org/10.1016/j.eiar.2023.107286.

Shi, Q., Liang, Q., Huo, T., You, K., Cai, W., 2023. Evaluation of CO2 and SO2 synergistic emission reduction: the case of China. J. Clean. Prod. 433 (October), 139784. https://doi.org/10.1016/j.jclepro.2023.139784.

Shi, R., Zhang, X., Zhu, Z., 2026. Greening firms through finance: how green finance drives corporate pollution and carbon reduction synergy in China. Int. Rev. Econ. Financ. 105 (July 2025), 104805. https://doi.org/10.1016/j.iref.2025.104805.

Su, P., Cong, X., Wang, L., Saparauskas, J., Ustinovi, L., 2025. Spatial network characteristics and influencing factors of the synergistic effects of pollution reduction and carbon emission reduction in "Zero Waste City" clusters. J. Clean. Prod. 493 (January).

Sun, B., Wang, M., Zhang, H., Zhao, Y., Li, X., 2025a. Assessing spatiotemporal trends and drivers of collaborative governance for air quality and carbon emission control: evidence from typical urban agglomerations in China. J. Clean. Prod. 519 (June), 146034. https://doi.org/10.1016/j.jclepro.2025.146034.

Sun, Z., Lu, Y., Zheng, X., Huang, Z., Yao, G., 2025b. Coupling coordination analysis of agricultural carbon reduction, pollution abatement, green expansion, and growth in Jiangsu Province, China. J. Agric. Food Res. 22 (March), 102098. https://doi.org/10.1016/j.jafr.2025.102098.

Tan, S., Xie, D., Ni, C., Zhao, G., Shao, J., Chen, F., Ni, J., 2023. Spatiotemporal characteristics of air pollution in Chengdu-Chongqing urban agglomeration (CCUA) in Southwest, China: 2015–2021. J. Environ. Manag. 325 (PA), 116503. https://doi.org/10.1016/j.jenvman.2022.116503.

Wang, J., Lu, X., Du, P., Zheng, H., Dong, Z., Yin, Z., Xing, J., Wang, S., Hao, J., 2022. The increasing role of synergistic effects in carbon mitigation and air quality improvement, and its associated health benefits in China. Engineering. https://doi.org/10.1016/j.eng.2022.06.004.

Wang, M., Lin, N., Dong, Y., Huang, X., Ma, Y., Tang, Y., Tao, X., Lu, X., 2023. The impact of farmland use transition on CO2 emissions and its spatial spillover effects from the perspective of major function-oriented zoning: the case of Huang-Huai-Hai plain. Environ. Impact Assess. Rev. 103 (April), 107254. https://doi.org/10.1016/j.eiar.2023.107254.

Wang, Z., Yu, Y., Zhou, R., 2024. A longitudinal exploration of the spatiotemporal coupling relationship and driving factors between regional urban development and ecological quality of green space. Ecol. Indic. 164 (May), 112134. https://doi.org/10.1016/j.ecolind.2024.112134.

Xian, B., Wang, Y., Xu, Y., Wang, J., Li, X., 2024. Assessment of the co-benefits of China's carbon trading policy on carbon emissions reduction and air pollution control in multiple sectors. Econ. Anal. Policy 81 (November 2023), 1322–1335. https://doi.org/10.1016/j.eap.2024.01.011.

Xiang, S., Huang, X., Lin, N., Yi, Z., 2025. Synergistic reduction of air pollutants and carbon emissions in Chengdu-Chongqing urban agglomeration, China: spatial-temporal characteristics, regional differences, and dynamic evolution. J. Clean. Prod. 493 (September 2024). https://doi.org/10.1016/j.jclepro.2025.144929.

Xiang, S., Huang, X., Ailin, A., Dong, Y., Li, M., Lin, N., 2026. Exploring carbon metabolism from perspective of land use in Chengdu-Chongqing urban agglomeration, China: a multi-scale and multi-scenario analysis framework. Cities 171 (January), 106773. https://doi.org/10.1016/j.cities.2026.106773.

Xie, P., Duan, Z., Wei, T., Pan, H., 2024. Spatial disparities and sources analysis of co-benefits between air pollution and carbon reduction in China. J. Environ. Manag. 354 (September 2023), 120433. https://doi.org/10.1016/j.jenvman.2024.120433.
Xu, J., Lv, T., Hou, X., Deng, X., Li, N., Liu, F., 2022. Spatiotemporal characteristics and influencing factors of renewable energy production in China: a spatial econometric analysis. Energy Econ. 116 (October). https://doi.org/10.1016/j.eneco.2022.106399.
Xu, Y., Liu, Z., Walker, T.R., Adams, M., Dong, H., 2024. Spatio-temporal patterns and spillover effects of synergy on carbon dioxide emission and pollution reductions in the Yangtze River Delta region in China. Sustain. Cities Soc. 107 (December 2023), 105419. https://doi.org/10.1016/j.scs.2024.105419.
Yan, R., Wang, H., Huang, C., An, J., Bai, H., Wang, Q., Gao, Y., Jing, S., Wang, Y., Su, H., 2024. Impact of spatial scales of control measures on the effectiveness of ozone pollution mitigation in eastern China. Sci. Total Environ. 906 (October 2023), 167521. https://doi.org/10.1016/j.scitotenv.2023.167521.
Yang, X., Ran, G., 2024. Factors influencing the coupled and coordinated development of cities in the Yangtze River Economic Belt: a focus on carbon reduction, pollution control, greening, and growth. J. Environ. Manag. 370 (August), 122499. https://doi.org/10.1016/j.jenvman.2024.122499.
Yang, T., Yi, L., Yan, S., Zhang, R., Wang, X., 2024. Synergy of pollution reduction and carbon abatement of the 8 urban agglomerations in China: status, dynamic evolution, and spatial-temporal characteristics. Res. Policy 95 (28), 105180. https://doi.org/10.1016/j.resourpol.2024.105180.
Yang, H., Shao, H., Zhang, C., Zhang, C., Su, W., Zhao, Q., 2025. Optimization framework for coupled and coordinated development of ecological environment and urbanization in dual-core urban agglomerations: a case study area of Chengdu-Chongqing. Ecol. Indic. 176 (May), 113624. https://doi.org/10.1016/j.ecolind.2025.113624.
Ye, W.F., Ma, Z.Y., Ha, X.Z., Yang, H.C., Weng, Z.X., 2018. Spatiotemporal patterns and spatial clustering characteristics of air quality in China: a city level analysis. Ecol. Indic. 91 (October 2017), 523–530. https://doi.org/10.1016/j.ecolind.2018.04.007.
Yi, M., Guan, Y., Wu, T., Wen, L., Selena, M., 2023. Assessing China's synergistic governance of emission reduction between pollutants and CO_2. Environ. Impact Assess. Rev. 102 (December 2022), 107196. https://doi.org/10.1016/j.eiar.2023.107196.
Yu, K., Li, Z., 2025. Multi-scenario analysis of green water resource efficiency under carbon emission constraints in the Chengdu-Chongqing urban agglomeration, China: a system dynamics approach. Ecol. Indic. 171 (December 2024), 113139. https://doi.org/10.1016/j.ecolind.2025.113139.
Zaller, J.G., Kruse-Plaß, M., Schlechtriemen, U., Gruber, E., Peer, M., Nadeem, I., Formayer, H., Hutter, H.P., Landler, L., 2023. Unexpected air pollutants with potential human health hazards: nitrification inhibitors, biocides, and persistent organic substances. Sci. Total Environ. 862 (October 2022), 0–5. https://doi.org/10.1016/j.scitotenv.2022.160643.
Zeng, Q.H., He, L.Y., 2023. Study on the synergistic effect of air pollution prevention and carbon emission reduction in the context of "dual carbon": evidence from China's transport sector. Energy Policy 173 (December 2022), 113370. https://doi.org/10.1016/j.enpol.2022.113370.
Zeng, L., Yang, B., Xiao, S., Yan, M., Cai, Y., Liu, B., Zheng, X., Wu, Y., 2022. Species profiles, in-situ photochemistry and health risk of volatile organic compounds in the gasoline service station in China. Sci. Total Environ. 842 (June). https://doi.org/10.1016/j.scitotenv.2022.156813.
Zhang, B., Wang, Q., Wang, S., Tong, R., 2023a. Coal power demand and paths to peak carbon emissions in China: a provincial scenario analysis oriented by CO2-related health co-benefits. Energy 282 (October 2022), 128830. https://doi.org/10.1016/j.energy.2023.128830.
Zhang, Y., Shi, M., Chen, J., Fu, S., Wang, H., 2023b. Spatiotemporal variations of NO2 and its driving factors in the coastal ports of China. Sci. Total Environ. 871 (2), 162041. https://doi.org/10.1016/j.scitotenv.2023.162041.
Zhang, J., Li, J., Su, Y., Chen, C., Chen, L., Huang, X., Wang, F., Huang, Y., Wang, G., 2024. Interannual evolution of the chemical composition, sources and processes of PM2.5 in Chengdu, China: insights from observations in four winters. J. Environ. Sci. (China) 138, 32–45. https://doi.org/10.1016/j.jes.2023.02.055.
Zhang, J., Lu, H., Peng, W., Zhang, L., 2025a. Analyzing carbon emissions and influencing factors in Chengdu-Chongqing urban agglomeration counties. J. Environ. Sci. (China) 151, 640–651. https://doi.org/10.1016/j.jes.2024.04.019.
Zhang, X., Wei, Y., Wang, T., Shen, J., Zhao, T., 2025b. Spatial correlation network on synergy between carbon reduction and pollution control in key areas for air pollution prevent and control. J. Clean. Prod. 491 (January), 144777. https://doi.org/10.1016/j.jclepro.2025.144777.
Zhang, X., Yin, S., Lu, X., Liu, Y., Wang, T., 2025c. Establish of air pollutants and greenhouse gases emission inventory and co-benefits of their reduction of transportation sector in Central China. J. Environ. Sci. 150, 604–621. https://doi.org/10.1016/j.jes.2023.12.025.
Zhao, R., Hu, C., Du, C., Wang, C., Sun, L., 2025. Synergistic effect assessment of pollution and carbon reduction and pathway of green transformation at regional level in China. J. Clean. Prod. 495 (February), 145013. https://doi.org/10.1016/j.jclepro.2025.145013.
Zou, C., Wu, L., Wang, Y., Sun, S., Wei, N., Sun, B., Ni, J., He, J., Zhang, Q., Peng, J., Mao, H., 2023. Evaluating traffic emission control policies based on large-scale and real-time data: a case study in central China. Sci. Total Environ. 860 (November 2022), 160435. https://doi.org/10.1016/j.scitotenv.2022.160435.